

Inferring Outcome Means of Exponential Family Distributions Estimated by Deep Neural Networks

Xuran Meng* and Yi Li†

Abstract

While deep neural networks (DNNs) are widely used for prediction, inference on DNN-estimated subject-specific means for categorical or exponential family outcomes remains underexplored. We address this by proposing a DNN estimator under generalized nonparametric regression models (GNRMs) and developing a rigorous inference framework. Unlike existing approaches that assume independence between prediction errors and inputs to establish the error bound, a condition often violated in GNRMs, we allow for dependence and our theoretical analysis demonstrates the feasibility of drawing inference under GNRMs. To implement inference, we consider an Ensemble Subsampling Method (ESM) that leverages U-statistics and the Hoeffding decomposition to construct reliable confidence intervals for DNN estimates. We show that, under GNRM settings, ESM enables model-free variance estimation and accounts for heterogeneity among individuals in the population. Through simulations under nonparametric logistic, Poisson, and binomial regression models, we demonstrate the effectiveness and efficiency of our method. We further apply the method to the electronic Intensive Care Unit (eICU) dataset, a large-scale collection of anonymized health records from ICU patients, to predict ICU readmission risk and offer patient-centric insights for clinical decision-making.

1 Introduction

In supervised learning (Hastie et al., 2009), the focus is often on the estimation of the conditional expectation $\mathbb{E}[y|\mathbf{x}]$, which represents the optimal prediction of the target variable y given covariates \mathbf{x} . The notion is fundamental because for a pair (\mathbf{x}, y) , the conditional expectation satisfies:

$$\mathbb{E}[\ell(y, y(\mathbf{x}))] \geq \mathbb{E}[\ell(y, \mathbb{E}[y|\mathbf{x}])]$$

for any predictor $y(\mathbf{x})$, where the loss function $\ell(y, y(\mathbf{x}))$ measures the discrepancy between the true label y and the prediction $y(\mathbf{x})$. Numerous methods have been developed to estimate $\mathbb{E}[y|\mathbf{x}]$, including linear, parametric and nonparametric regression, kernel regression (Nadaraya, 1964), support vector regression (Drucker et al., 1996), and deep neural networks (LeCun et al., 2015).

Deep neural networks (DNNs) present remarkable capabilities in modeling $\mathbb{E}[y|\mathbf{x}]$, and often outperform traditional techniques in accuracy and scalability. However, the statistical inference surrounding the estimation of $\mathbb{E}[y|\mathbf{x}]$, especially when y is categorical or belongs to the exponential family, remains underdeveloped. We aim to address this gap by establishing a rigorous framework for statistical inference on $\mathbb{E}[y|\mathbf{x}]$ estimated by DNNs under a generalized nonparametric regression model (GNRM) setting [see Eq. (2.3)].

*Department of Biostatistics, University of Michigan; e-mail: xuranm@umich.edu

†Department of Biostatistics, University of Michigan; e-mail: yili@umich.edu

Modern inference approaches include distribution-free conformal prediction inference (Lei et al., 2018; Angelopoulos and Bates, 2021; Huang et al., 2024), extensions of jackknife inference within conformal prediction (Alaa and Van Der Schaar, 2020; Kim et al., 2020; Barber et al., 2021), debiasing methods (Athey et al., 2018; Guo et al., 2021), residual-based bootstrap techniques (Zhang and Politis, 2023), and the use of U statistics in regressions, random forests and neural networks (Mentch and Hooker, 2016; Wager and Athey, 2018; Schupbach et al., 2020; Wang and Wei, 2022; Fei and Li, 2024). Several limitations remain. Conformal prediction, for example, provides prediction intervals under continuous regression settings by accounting for the randomness of both y and $\mathbb{E}[y|\mathbf{x}]$. However, the resulting intervals tend to be conservative, producing wide bounds and leading to reduced efficiency compared to methods that directly model the uncertainty of $\mathbb{E}[y|\mathbf{x}]$. Debiasing techniques such as those in (Athey et al., 2018; Guo et al., 2021) yield useful intervals, but are restricted to models with linear functions of \mathbf{x} , limiting their applicability to DNNs. Similarly, the residual bootstrap method proposed in (Zhang and Politis, 2023) is adapted to linear regression frameworks and does not readily extend to more complex prediction scenarios. Mentch and Hooker (2016) and Wager and Athey (2018) provided insights into quantifying prediction uncertainty for random forests, and Schupbach et al. (2020) explored U-statistics in neural networks, albeit with limited theoretical justification. Recently, Fei and Li (2024) examined U-statistics in neural networks rigorously, but their results remain tied to continuous outcomes, leaving open questions of whether these methods can be applied to GNRMs such as nonparametric logistic and Poisson regressions.

Theoretically, for valid inference on $\mathbb{E}[y|\mathbf{x}]$, we need to establish the convergence rate of neural networks in a GNNRM framework. Since the universal approximation theorem (Hornik et al., 1989), there has been substantial progress in understanding the convergence rates of neural networks; see McCaffrey and Gallant (1994); Kohler and Krzyżak (2005); Yarotsky (2017, 2018); Shen et al. (2019); Kohler and Langer (2021); Lu et al. (2021); Shen et al. (2021); Jiao et al. (2023); Yan and Yao (2023); Fan et al. (2024); Wang et al. (2024); Bhattacharya et al. (2024). For instance, Shen et al. (2021) established the convergence rate under nonparametric regression with the assumption p -th moment of response is bounded for some $p > 1$; Fan et al. (2024) explored nonasymptotic error bounds of the estimators under several loss functions, such as the least-absolute deviation loss and Huber loss; Wang et al. (2024) proposed an efficient and robust nonparametric regression estimator based on an estimated maximum likelihood estimator; Fan and Gu (2024); Bhattacharya et al. (2024) investigated deep neural network estimators for nonparametric interaction models with diverging input dimensions, focusing on theoretical properties such as minimax optimality, approximation error control, and sparsity-driven regularization. However, quantifying uncertainty of DNN-estimated $\mathbb{E}[y|\mathbf{x}]$ within the framework of GNNRM introduces additional challenges. The existing approaches typically assume a nonparametric regression framework, where the distribution of $y - \mathbb{E}[y|\mathbf{x}]$ is independent of the covariates \mathbf{x} . This assumption simplifies the theoretical analysis and the derivation of convergence results (Takezawa, 2005; Györfi et al., 2006; Fan, 2018). In generalized nonparametric regression settings, however, the assumption often fails as the distribution of $y - \mathbb{E}[y|\mathbf{x}]$ may still depend on \mathbf{x} . Consequently, the standard techniques for bounding error terms and controlling variance no longer apply, and the established results on uniform convergence or concentration inequalities (Bartlett et al., 2020) are invalid. As a result, it is unclear whether these methods are applicable for drawing inference on GNRMs estimated by DNNs.

Our contributions in addressing these challenges are as follows. First, we propose a DNN estimator for subject-specific means under GNRMs and develop a rigorous inference framework. To

establish the convergence rate — crucial for demonstrating the feasibility of using the estimator for both estimating f_0 and conducting inference — we account for the dependence of the distribution of $y - \mathbb{E}[y|\mathbf{x}]$ on \mathbf{x} , which arises from heteroskedasticity in GNRMs. We apply truncations to partition the analysis into bounded and unbounded noise regimes. Standard convergence results hold in the bounded regime, while in the unbounded regime, integral bounds and concentration inequalities ensure that extreme noise contributions are asymptotically negligible. This yields rigorous error bounds under general GNRM conditions. As opposed to [Schmidt-Hieber \(2020\)](#) that focused on continuous outcomes, our work accommodates a broader class of outcomes, both continuous and discrete, encompassing the work of ([Schmidt-Hieber, 2020](#)) as a special case. This demonstrates that similar principles can be extended to the wider GNRM framework. Second, to quantify the uncertainty of the estimates, we propose an ensemble subsampling method (ESM) under GNRMs, developed from U-statistics ([Frees, 1989](#); [Hoeffding, 1992](#); [Lee, 2019](#); [Boroskikh, 2020](#)) and Hoeffding decomposition ([Hoeffding, 1992](#)). Our model-free variance estimator leverages the intrinsic properties of Hoeffding decomposition and accommodates varying population levels as well as individual variance structures.

In [Section 2](#), we introduce deep neural networks (DNNs), generalized nonparametric regression models (GNRMs) and the ensemble subsampling method (ESM). [Section 3](#) presents theoretical results for the convergence rate of DNNs under the GNRM framework, as well as results for statistical inference using ESM. In [Section 4](#), we perform simulations to evaluate the finite sample performance of our method. [Section 5](#) applies the methodology to an electronic Intensive Care Unit (eICU) dataset to predict the number of ICU readmissions. The eICU dataset is a large-scale, multi-center dataset containing anonymized health data from ICU patients, as part of a collaboration between the Massachusetts Institute of Technology and several healthcare organizations. The results may inform identification of high-risk individuals, enabling caregivers to offer personalized care. [Section 6](#) concludes the paper with discussions. The proofs of the main theorems are given in [Appendix A](#), while additional numerical experiments and technical proofs are included in the Supplementary materials.

2 The Preamble

We employ lower letters (e.g. a) for scalars and boldface letters for vectors and matrices (e.g. \mathbf{a} and \mathbf{A}). For any matrix \mathbf{A} , we use $\|\mathbf{A}\|_0$ and $\|\mathbf{A}\|_\infty$ to denote its zero norm and infinity norm, respectively. The set of natural and real numbers are denoted by \mathbb{N} and \mathbb{R} respectively. For any function f mapping a vector to \mathbb{R} , we use $\|f\|_\infty$ to denote its infinity norm. For an integer n , $[n] = \{1, \dots, n\}$. We write $X_1(n) = O(X_2(n))$ or $X_1(n) \lesssim X_2(n)$ if for any $\varepsilon > 0$, there exists $C > 0$ such that $\mathbb{P}(|X_1(n)/X_2(n)| > C) \leq \varepsilon$ for all n . We denote $X_1(n) = o(X_2(n))$ if $\{X_1(n)/X_2(n)\}$ converges to 0 in probability, and $X_1(n) \sim X_2(n)$ if $\{X_1(n)/X_2(n)\}$ converges to 1 in probability. When clear from context, we use the same symbol for a random variable and its realized value to avoid redundancy.

2.1 Deep Neural Networks

Let L be a positive integer and $\mathbf{p} = (p_0, \dots, p_L, p_{L+1})^\top$ be a vector of positive integers. An $(L+1)$ -layer DNN with layer-width \mathbf{p} is defined as

$$f(\mathbf{x}) = \mathbf{W}_L f_L(\mathbf{x}) + \mathbf{v}_L, \quad (2.1)$$

with the recursive expression

$$f_l(\mathbf{x}) = \sigma(\mathbf{W}_{l-1}f_{l-1}(\mathbf{x}) + \mathbf{v}_{l-1}), \quad f_1(\mathbf{x}) = \sigma(\mathbf{W}_0\mathbf{x} + \mathbf{v}_0).$$

Here, $\mathbf{W}_l \in \mathbb{R}^{p_{l+1} \times p_l}$ and vectors $\mathbf{v}_l \in \mathbb{R}^{p_{l+1}}$ ($l \in [L]$) are the parameters of this DNN, and $\sigma : \mathbb{R} \rightarrow \mathbb{R}$, an activation function, is applied element-wise to vectors. A commonly used activation function is the rectified linear unit (ReLU) function (Nair and Hinton, 2010), or $\sigma(x) = \max(x, 0)$. We focus on it due to its piecewise linearity and projection properties, with potential extensions to other activation functions as discussed in Section 6. In (2.1), L denotes the **depth** of the neural network, \mathbf{p} specifies the **width** of each layer, with p_0 corresponding to the input dimension, p_1, \dots, p_L the dimensions of the L hidden layers, and p_{L+1} the dimension of the output layer.

Fully connected DNNs have a large number of parameters, which can lead to overfitting by making the network memorize training data rather than generalize. Introducing sparsity and boundedness reduces model complexity and improves generalization. We focus on the following class of s -sparse and F -bounded networks for our theoretical analysis:

$$\mathcal{F}(L, \mathbf{p}, s, F) = \left\{ f \text{ of form (2.1): } \|\mathbf{W}_l\|_\infty, \|\mathbf{v}_l\|_\infty \leq 1, \sum_{l=1}^L \|\mathbf{W}_l\|_0 + \|\mathbf{v}_l\|_0 \leq s, \|f\|_\infty \leq F \right\}. \quad (2.2)$$

Here, $s \in \mathbb{N}_+$, and $F > 0$ is a constant. $\|\cdot\|_0$ is the number of nonzero entries of matrix or vector, and $\|f\|_\infty$ is the sup-norm of function f .

2.2 Generalized Nonparametric Regression

We consider outcomes from the exponential family, encompassing widely used distributions such as the normal, Bernoulli, Poisson, and binomial. For a random variable y belonging to the exponential family, its probability density (or mass) function is given by

$$p(y|\theta) = h(y) \exp \{ \theta y - \psi(\theta) \},$$

where θ is the natural parameter, $h(y)$ is the base measure, and $\psi(\theta)$ is the log-partition function to ensure normalization. Following Fei and Li (2021), we have omitted the dispersion parameter for simplicity, as it does not impact the estimation of the means in our cases.

Suppose we observe n independently and identically distributed (iid) sample $\{(\mathbf{x}_i, y_i)\}_{i=1}^n$ from (\mathbf{x}, y) , where $\mathbf{x} \in \mathbb{R}^p$ is a covariate vector and $y \in \mathbb{R}$ is the response variable. Given \mathbf{x} , the distribution of y is modeled as

$$p(y|\mathbf{x}) = h(y) \exp \left\{ y f_0(\mathbf{x}) - \psi(f_0(\mathbf{x})) \right\}, \quad (2.3)$$

where $f_0 : \mathbb{R}^d \rightarrow \mathbb{R}$ is the nonparametric function linking \mathbf{x} to θ . Model (2.3) is referred to as a Generalized Nonparametric Regression Model (GNRM), where the outcomes follow a distribution from the exponential family. To predict y_{new} given a new test point \mathbf{x}_{new} , a natural choice is $\mathbb{E}(y_{\text{new}}|\mathbf{x}_{\text{new}}) = \psi'(f_0(\mathbf{x}_{\text{new}}))$, where the inverse of function $\psi'(\cdot)$ is commonly known as the link function. Consequently, it is of interest to estimate f_0 . By the universal approximation theorem (Hornik et al., 1989), deep neural networks are suitable candidates for estimating f_0 . We propose a DNN estimator, \hat{f}_n^* , which minimizes the negative log likelihood function (2.3) over the class of

DNNs defined in (2.2), that is,

$$\hat{f}_n^* = \operatorname{argmin}_{f \in \mathcal{F}(L, \mathbf{p}, s, F)} \frac{1}{n} \sum_{i=1}^n \{-y_i f(\mathbf{x}_i) + \psi(f(\mathbf{x}_i))\}. \quad (2.4)$$

The estimator (2.4) is applicable to commonly used models, including these listed below.

Nonparametric Gaussian Regression: Given \mathbf{x} , we assume that the response variable follows a Gaussian distribution with mean $f_0(\mathbf{x})$ and variance σ^2 . In this setting, the variance parameter σ^2 does not affect the estimation of the mean function $f_0(\mathbf{x})$, which can be seen by examining the likelihood and optimization. The likelihood function for a nonparametric Gaussian regression model is given by $p(y|\mathbf{x}) = \frac{1}{\sqrt{2\pi}\sigma} e^{-\frac{(y-f_0(\mathbf{x}))^2}{2\sigma^2}}$. An application of (2.4) to this setting yields:

$$\begin{aligned} \hat{f}_n^* &= \operatorname{argmin}_{f \in \mathcal{F}(L, \mathbf{p}, s, F)} \frac{1}{n} \sum_{i=1}^n \{-y_i f(\mathbf{x}_i) + \frac{1}{2} f^2(\mathbf{x}_i)\} \\ &= \operatorname{argmin}_{f \in \mathcal{F}(L, \mathbf{p}, s, F)} \frac{1}{n} \sum_{i=1}^n \{y_i - f(\mathbf{x}_i)\}^2, \end{aligned}$$

which corresponds to minimizing the empirical mean squared error (MSE), as considered by [Schmidt-Hieber \(2020\)](#).

Nonparametric Logistic Regression: To model binary outcomes, we set $h(y) = 1$, $\psi(\theta) = \log(1 + e^\theta)$ in (2.3), and let $y \in \{0, 1\}$. The estimator (2.4) in this setting can be written as:

$$\hat{f}_n^* = \operatorname{argmin}_{f \in \mathcal{F}(L, \mathbf{p}, s, F)} \frac{1}{n} \sum_{i=1}^n (-y_i f(\mathbf{x}_i) + \log[1 + \exp\{f(\mathbf{x}_i)\}]).$$

Nonparametric Poisson Regression: Considering $y \in \mathbb{N}$ (non-negative integers), we define $h(y) = \frac{1}{y!}$ and $\psi(\theta) = e^\theta$ in (2.3). The estimator (2.4) has the following form:

$$\hat{f}_n^* = \operatorname{argmin}_{f \in \mathcal{F}(L, \mathbf{p}, s, F)} \frac{1}{n} \sum_{i=1}^n [\exp\{f(\mathbf{x}_i)\} - y_i f(\mathbf{x}_i)].$$

Nonparametric Binomial Regression: Consider that, given covariates \mathbf{x} , the response variable y follows a Binomial distribution with a fixed number of trials n_{trial} and the success probability $p(\mathbf{x}) = \frac{1}{1 + e^{-f_0(\mathbf{x})}}$. This corresponds to $h(y) = \binom{n_{\text{trial}}}{y}$ and $\psi(\theta) = n_{\text{trial}} \log(1 + e^\theta)$. In this setting, the estimator (2.4) is specified as

$$\hat{f}_n^* = \operatorname{argmin}_{f \in \mathcal{F}(L, \mathbf{p}, s, F)} \frac{1}{n} \sum_{i=1}^n \left[-y_i f(\mathbf{x}_i) + n_{\text{trial}} \log\{1 + e^{f(\mathbf{x}_i)}\} \right].$$

2.3 Approximate Empirical Risk Minimization and Function Smoothness

As the DNN estimator (2.4) is an approximate empirical loss minimizer, we use the following $\Delta_n(\hat{f}_n, f_0)$ to measure the difference between the expected empirical risk of \hat{f}_n and the global

minimum over all networks in the class, that is,

$$\Delta_n(\hat{f}_n, f_0) = \mathbb{E}_{f_0} \left\{ \frac{1}{n} \sum_{i=1}^n -y_i \hat{f}_n(\mathbf{x}_i) + \psi(\hat{f}_n(\mathbf{x}_i)) - \inf_{f \in \mathcal{F}(L, \mathbf{p}, s, \mathcal{F})} \frac{1}{n} \sum_{i=1}^n -y_i f(\mathbf{x}_i) + \psi(f(\mathbf{x}_i)) \right\}. \quad (2.5)$$

Obviously, $\Delta_n(\hat{f}_n, f_0) = 0$ if \hat{f}_n is an empirical risk minimizer. We also define

$$\ell(\mathbf{x}; \hat{f}_n, f_0) = -\psi'(f_0(\mathbf{x}))\hat{f}_n(\mathbf{x}) + \psi(\hat{f}_n(\mathbf{x})) + \psi'(f_0(\mathbf{x}))f_0(\mathbf{x}) - \psi(f_0(\mathbf{x})),$$

which measures the discrepancy between the predictor \hat{f}_n and the true function f_0 at a point \mathbf{x} outside the training sample, $(\mathbf{x}_i, y_i)_{i=1}^n$. The prediction error $R_n(\hat{f}_n, f_0)$ is then defined as the expected value of the loss function:

$$R_n(\hat{f}_n, f_0) := \mathbb{E}[\ell(\mathbf{X}; \hat{f}_n, f_0)], \quad (2.6)$$

where \mathbf{X} is an out of sample point such that $\mathbf{X} \stackrel{\mathcal{D}}{=} \mathbf{x}_1$ and is independent of $(\mathbf{x}_i, y_i)_{i=1}^n$.

For desirable properties of \hat{f}_n , we assume that f_0 belongs to a Hölder class of smooth functions. This assumption provides a flexible framework for characterizing function smoothness, which is important for establishing convergence rates, consistency, and estimator optimality. It allows the use of approximation theory and functional analysis to derive meaningful statistical guarantees. Widely adopted in the literature (Schmidt-Hieber, 2020; Zhong et al., 2022; Fan and Gu, 2024), the Hölder class of smooth functions with parameters γ , $K > 0$, and domain $\mathbb{D} \subset \mathbb{R}^r$ is

$$\mathcal{G}_r^\gamma(\mathbb{D}, K) = \left\{ g : \mathbb{D} \rightarrow \mathbb{R} : \sum_{\beta: \|\beta\|_1 < \gamma} \|\partial^\beta g\|_\infty + \sum_{\beta: \|\beta\|_1 = \lfloor \gamma \rfloor} \sup_{\mathbf{x}, \mathbf{y} \in \mathbb{D}, \mathbf{x} \neq \mathbf{y}} \frac{|\partial^\beta g(\mathbf{x}) - \partial^\beta g(\mathbf{y})|}{\|\mathbf{x} - \mathbf{y}\|_\infty^{\gamma - \lfloor \gamma \rfloor}} \leq K \right\},$$

where $\lfloor \gamma \rfloor$ is the largest integer strictly smaller than γ , and $\partial^\beta = \partial^{\beta_1} \dots \partial^{\beta_r}$ with $\beta = (\beta_1, \dots, \beta_r)^\top \in \mathbb{N}^r$. We further assume that the nonparametric function f_0 is a $(q+1)$ -composition ($q \in \mathbb{N}$) of several functions, that is for some vectors $\mathbf{d} = (d_0, \dots, d_{q+1}) \in \mathbb{N}_+^{q+2}$, $\mathbf{t} = (t_0, \dots, t_q) \in \mathbb{N}_+^{q+1}$ and $\gamma = (\gamma_0, \dots, \gamma_q) \in \mathbb{R}_+^{q+1}$, $f_0 \in \mathcal{G}(q, \mathbf{d}, \mathbf{t}, \gamma, K)$, where

$$\mathcal{G}(q, \mathbf{d}, \mathbf{t}, \gamma, K) := \left\{ f = g_q \circ \dots \circ g_0 : g_i = (g_{ij})_j : [a_i, b_i]^{d_i} \rightarrow [a_{i+1}, b_{i+1}]^{d_{i+1}}, \right. \\ \left. g_{ij} \in \mathcal{G}_{t_i}^{\gamma_i}([a_i, b_i]^{t_i}) \text{ with } |a_i|, |b_i| \leq K \right\},$$

and \mathbf{d} and \mathbf{t} characterize the dimensions of the function, while γ represents the measure of smoothness. For instance, if

$$f_0(\mathbf{x}) = g_{21} \left(g_{11}(g_{01}(x_1, x_2, x_3, x_4), g_{02}((x_5, x_6, x_7, x_8))), \right. \\ \left. g_{12}(g_{03}(x_9, x_{10}, x_{11}, x_{12}), g_{04}((x_{13}, x_{14}, x_{15}, x_{16}))), \right. \\ \left. g_{13}(g_{05}(x_{17}, x_{18}, x_{19}, x_{20}), g_{06}((x_{21}, x_{22}, x_{23}, x_{24}))) \right), \quad \mathbf{x} \in [0, 1]^{24},$$

and g_{ij} are twice continuously differentiable, then smoothness $\gamma = (2, 2, 2)$, dimensions $\mathbf{d} = (24, 6, 3, 1)^\top$ and $\mathbf{t} = (4, 2, 3)^\top$. We further define $\gamma_j^* = \gamma_j \prod_{l=i+1}^q (\gamma_l \wedge 1)$ and $\phi_n = \max_{j=0, \dots, q} n^{-\frac{2\gamma_j^*}{2\gamma_j^* + t_j}}$.

2.4 Ensemble Subsampling Method (ESM)

Consider a scenario where \mathbf{x} is drawn from an unknown probability measure $\mathbb{P}_{\mathbf{x}}$ supported on \mathcal{X} , and for an input $\mathbf{x}_{\text{new}} = \mathbf{x}_* \in \mathcal{X}$, the unobserved outcome y_{new} follows (2.3). Our goal is to predict the conditional expectation $\mathbb{E}(y_{\text{new}}|\mathbf{x}_{\text{new}} = \mathbf{x}_*) = \psi'(f_0(\mathbf{x}_*))$ along with its uncertainty. For this, we introduce the Ensemble Subsampling Method (ESM), based on subsampling techniques (Wager and Athey, 2018; Fei and Li, 2024), to construct ensemble predictors and confidence intervals. ESM consists of the following components:

- (Subsampling) Let $\mathcal{I} = \{1, \dots, n\}$ denote the index set of the training dataset \mathcal{D}_n . We construct subsets of size $r(< n)$, yielding $B^* = \binom{n}{r}$ unique combinations. Denoting the b -th subset as $\mathcal{I}^b = \{i_1, \dots, i_r\}$, where $i_1 < \dots < i_r$ and $b \in [1 : B^*]$.
- (Predictor Construction) For each subset \mathcal{I}^b , the model is trained using the observations indexed by \mathcal{I}^b . The corresponding predictor $\hat{f}^b \in \mathcal{F}(L, \mathbf{p}, s, F)$ is obtained by solving the optimization problem:

$$\hat{f}^b = \operatorname{argmin}_{f \in \mathcal{F}(L, \mathbf{p}, s, F)} \frac{1}{|\mathcal{I}^b|} \sum_{i \in \mathcal{I}^b} -y_i f(\mathbf{x}_i) + \psi(f(\mathbf{x}_i)).$$

- (Ensemble Prediction) Using the predictors $\{\hat{f}^b : b = 1, \dots, B^*\}$, we compute the ensemble prediction for any $\mathbf{x}_* \in \mathcal{X}$ as:

$$\hat{f}^{B^*}(\mathbf{x}_*) = \frac{1}{B^*} \sum_{b=1}^{B^*} \hat{f}^b(\mathbf{x}_*),$$

The conditional expectation is then estimated as $\mathbb{E}(y_{\text{new}}|\mathbf{x}_{\text{new}} = \mathbf{x}_*) = \psi'(\hat{f}^{B^*}(\mathbf{x}_*))$.

- (Confidence Interval Construction) To quantify uncertainty, we estimate the variance, denoted $\hat{\sigma}_*$, using the infinitesimal jackknife method. The resulting confidence interval (CI) is defined as:

$$\text{CI}(\mathbf{x}_*) = [\psi'(\hat{f}^{B^*}(\mathbf{x}_*) - c_\alpha \hat{\sigma}_*), \psi'(\hat{f}^{B^*}(\mathbf{x}_*) + c_\alpha \hat{\sigma}_*)]. \quad (2.7)$$

where c_α is a constant controlling the $1 - \alpha$ confidence level.

The distribution of $\hat{f}^b(\mathbf{x}_*)$ for a fixed \mathbf{x}_* is intractable. However, since $\hat{f}^b(\mathbf{x}_*)$ is permutation symmetric with respect to \mathcal{I}^b , the ensemble predictor $\hat{f}^{B^*}(\mathbf{x}_*)$ forms a generalized U-statistic, which we later show to be asymptotically normal by leveraging U-statistics theory. In practice, we allow r to grow with n , but evaluating all $B^* = \binom{n}{r}$ models becomes computationally infeasible. To overcome this, we use a stochastic approximation by randomly drawing B size- r subsamples from \mathcal{D}_n . This involves independently sampling indices b_1, \dots, b_B from 1 to $\binom{n}{r}$, where each subsample is indexed by \mathcal{I}^{b_j} . The estimator $\hat{f}^B(\mathbf{x}_*)$ is defined as

$$\hat{f}^B(\mathbf{x}_*) = \frac{1}{B} \sum_{j=1}^B \hat{f}^{b_j}(\mathbf{x}_*). \quad (2.8)$$

As (2.8) provides the predictor for f_0 , the variance $\hat{\sigma}_*$ in (2.7) in the Confidence Interval Construc-

tion procedure is given as

$$\hat{\sigma}_*^2 = \frac{n(n-1)}{(n-r)^2} \sum_{i=1}^n \hat{V}_i^2. \quad (2.9)$$

Here, \hat{V}_i is defined as

$$\hat{V}_i = \frac{\sum_{j=1}^B (J_{b_j i} - J_{\cdot i}) (\hat{f}^{b_j}(\mathbf{x}_*) - \hat{f}^B(\mathbf{x}_*))}{B},$$

where $J_{b_j i} = I(i \in \mathcal{I}^{b_j})$ and $J_{\cdot i} = \frac{1}{B} \sum_{j=1}^B J_{b_j i}$.

3 Theoretical Results

We study the asymptotic properties of the ensemble predictor \hat{f}_n^B in (2.8). We first impose some regularity assumptions.

Assumption 3.1. *Suppose that (2.3) holds. The support of y , denoted by $\text{supp}(h(y))$ is fixed and does not depend on $f_0(\mathbf{x})$. In other words, $h(y) > 0$ for all $y \in \text{supp}(h)$. Moreover, the sufficient statistic $T(y) = y$ is not degenerate and can take at least two distinct values in $\text{supp}(h)$.*

Assumption 3.2. *For any \mathbf{x} , the conditional distribution $p(y|\mathbf{X} = \mathbf{x})$ is sub-exponential. Specifically, there exists a universal constant $\kappa > 0$ such that for all $t > 0$,*

$$\mathbb{P}(|y - \mathbb{E}[y|\mathbf{X} = \mathbf{x}]| \geq t | \mathbf{X} = \mathbf{x}) \leq 2 \exp\left(-\frac{t}{\kappa}\right).$$

Assumption 3.3. *The network class $\mathcal{F}(L, \mathbf{p}, s, F)$ with L , \mathbf{p} and s satisfies*

1. $F \geq \max(K, 1)$,
2. $\sum_{i=0}^q \log_2(4t_i \vee 4\gamma_i) \log_2 n \leq L \lesssim \log^\alpha n$ for some $\alpha > 1$,
3. $n\phi_n \lesssim \min_{i=1, \dots, L} p_i \leq \max_{i=1, \dots, L} p_i \lesssim n$,
4. $s \lesssim n\phi_n \log n$.

Assumption 3.1 is mild, ensuring that $p(y|\mathbf{X} = \mathbf{x})$ remains well-defined and avoids collapsing into a degenerate distribution. Additionally, that $T(y) = y$ takes at least two distinct values in $\text{supp}(h)$ guarantees a non-zero variance of y , ensuring the log-partition function $\psi(f_0(\mathbf{x}))$ exhibits local convexity. Assumption 3.2 is technical and ensures the concentration of the label variable Y does not deviate too much. Assumptions 3.1 and 3.2 are satisfied by most common exponential family distributions, such as χ_K^2 with fixed K , Beta, Bernoulli, Poisson, and Gaussian distributions, making them broadly applicable. Assumption 3.3 is a technical assumption, which specifies the requirements on the network parameters relative to the sample size n and smoothness parameters ϕ_n , t_i and γ_i , including the number of layers L and the sparsity s .

We let $\mathbf{z}_i = (y_i, \mathbf{x}_i)$ represent an independent observation of sample points. To further investigate the asymptotic properties of \hat{f}_n^B , we introduce

$$\xi_{1,r}(\mathbf{x}) = \text{Cov}(\hat{f}(\mathbf{x}; \mathbf{z}_1, \mathbf{z}_2, \dots, \mathbf{z}_r), \hat{f}(\mathbf{x}, \mathbf{z}_1, \mathbf{z}_2', \dots, \mathbf{z}_r')),$$

where $\mathbf{x} \in \mathcal{X}$ is in the support of probability measure $\mathbb{P}_{\mathbf{x}}$, and $\xi_{1,r}$ quantifies the covariance between predictions based on two overlapping subsets of size r that share a common point \mathbf{z}_1 but differ in the remaining elements. This term represents a second-order component in the Hoeffding decomposition of a U-statistic (Hoeffding, 1992), capturing the pairwise dependence structure within the subsamples used for constructing the estimator. Here, $\widehat{f}(\mathbf{x}; \mathbf{z}_1, \mathbf{z}_2, \dots, \mathbf{z}_r)$ means that we obtain \widehat{f} from the subsample $\mathbf{z}_1, \mathbf{z}_2, \dots, \mathbf{z}_r$, and then apply it to the point \mathbf{x} . The terms \mathbf{z}'_i and \mathbf{z}_i are independently generated from the same data generation process.

Assumption 3.4. *The covariance $\xi_{1,r}(\mathbf{x})$ for any given \mathbf{x} satisfies $\lim_{n \rightarrow \infty} 1/(n \inf_{\mathbf{x} \in \mathcal{X}} \xi_{1,r}(\mathbf{x})) = 0$. The sub sampling size r satisfies $\lim_{n \rightarrow \infty} r/n = 0$ and $\lim_{n \rightarrow \infty} n\phi_r L \log^2(r)/(r^2 \inf_{\mathbf{x} \in \mathcal{X}} \xi_{1,r}(\mathbf{x})) = 0$. Here, $\phi_r = \max_{j=0, \dots, q} r^{-(2\gamma_j^*)/(2\gamma_j^* + t_j)}$. Furthermore, the number of subsampling times B is large such that $\lim_{n \rightarrow \infty} n/B = 0$.*

Assumption 3.4 gives assumptions on the covariance $\xi_{1,r}(\mathbf{x})$, the subsample size r , total sample size n , and number of subsampling repetitions B . It allows some degeneracy in the first-order U-statistic covariance but ensures its rate remains above n^{-1} to keep the first-order contribution identifiable. The condition $\lim_{n \rightarrow \infty} n\phi_r L \log^2(r)/(r^2 \inf_{\mathbf{x} \in \mathcal{X}} \xi_{1,r}(\mathbf{x})) = 0$ is a necessary lower bound on r to guarantee sufficient training information per subsample. It indicates that a sufficiently large r is required to ensure deep neural networks learn f_0 effectively; one example is $r = n\phi_n$. A large enough B minimizes subsampling noise, preserving the estimator's asymptotic behavior and accuracy by keeping variability from limited subsamples negligible.

Theorem 3.5. *Suppose that $f_0 \in \mathcal{G}(q, \mathbf{d}, \mathbf{t}, \gamma, K)$ and $\widehat{f}_n \in \mathcal{F}(L, \mathbf{p}, s, F)$. If Assumptions 3.1-3.3 hold, then it holds that*

$$\frac{1}{2} \Delta_n(\widehat{f}_n, f_0) - c' \phi_n L \log^2 n \leq R_n(\widehat{f}_n, f_0) \leq 2 \Delta_n(\widehat{f}_n, f_0) + C' \phi_n L \log^2 n.$$

for some constants $c', C' > 0$. Here, $\Delta_n(\widehat{f}_n, f_0)$ is defined in (2.5).

Theorem 3.5 establishes a bound on the out-of-sample estimation error. Unlike previous studies (Schmidt-Hieber, 2020; Fan and Gu, 2024), which primarily focus on bounding the in-sample mean squared error (MSE), i.e., $\frac{1}{n} \sum_{i=1}^n (y_i - f(\mathbf{x}_i))^2$, to derive bounds for the prediction error, our approach applies to a wide class of training losses (2.5) under GNRMs. The heteroskedasticity inherent in GNRMs necessitates a more refined analysis, and a truncation technique is introduced to address this challenge by separating the noise into different regimes. Specifically, this result enables the analysis of non-Gaussian outcomes with heteroskedasticity even depends on covariates, overcoming key limitations of prior methods (Schmidt-Hieber, 2020; Fan and Gu, 2024) that rely on the independence of $y_i - \mathbb{E}(y_i|\mathbf{x}_i)$ and $f_0(\mathbf{x}_i)$ to derive prediction error bounds. Theorem 3.5 also implies that the aggregated estimator \widehat{f}^B has a vanishing bias, as shown in the following corollary.

Corollary 3.6. *Assume that the conditions of Theorem 3.5 hold, Assumption 3.3 holds for the sub sample size r , the neural network fitted on sub samples belongs to $\mathcal{F}(L, \mathbf{p}, s, F)$, $\Delta_n(\widehat{f}^{b_j}, f_0) \leq C\phi_r L \log^2 r$, and Assumption 3.4 holds. Then for a new independent and identical random variable $\mathbf{X} \sim \mathbb{P}_{\mathbf{x}}$, it holds that*

$$\frac{n}{r^2 \inf_{\mathbf{x} \in \mathcal{X}} \xi_{1,r}(\mathbf{x})} \cdot \mathbb{E}|\mathbb{E}(\widehat{f}^B(\mathbf{X}) - f_0(\mathbf{X})|\mathbf{X})|^2 \rightarrow 0.$$

Corollary 3.6 implies asymptotic unbiasedness, i.e., $\mathbb{E}\{\hat{f}^B(\mathbf{X})|\mathbf{X}\} = f_0(\mathbf{X}) + o_p\left(\sqrt{\frac{r^2\xi_{1,r}(\mathbf{X})}{n}}\right)$.

That is, the first-order term in the Hoeffding decomposition of \hat{f}^B is asymptotically negligible. As a result, the second-order term characterized by a normal distribution dominates, and we can establish the asymptotic normality of \hat{f}^B as stated in Theorem 3.7. The lower bound of r implied by Assumption 3.4 ensures that the bias of $\mathbb{E}\{\hat{f}^B(\mathbf{X})|\mathbf{X}\}$ is asymptotically negligible, at least in the L_2 sense. In contrast, if r is relatively small, the bias of \hat{f}^B may be large, and this is further verified by our simulations.

Theorem 3.7. *Suppose that the data \mathcal{D}_n are generated from Model (2.3) with an unknown $f_0 \in \mathcal{G}(q, \mathbf{d}, \mathbf{t}, \gamma, K)$, the used neural networks belong to $\mathcal{F}(L, \mathbf{p}, s, F)$, $\Delta_n(\hat{f}^{b_j}, f_0) \leq C\phi_r L \log^2 r$ for all subsample sets, Assumptions 3.1, 3.2 and 3.4 hold, and Assumption 3.3 holds for the subsample size r . Then there exists positive sequence, $\delta_1, \delta_2, \dots$, with $\delta_n \rightarrow 0$ and corresponding set $\mathcal{A}_{\delta_n} \subseteq \mathcal{X}$ with $\mathbb{P}_{\mathbf{X}}(\mathcal{A}_{\delta_n}) \geq 1 - \delta_n$, such that for any fixed $\mathbf{x}_* \in \mathcal{A}_{\delta_n}$, the predictor $\hat{f}^B(\mathbf{x}_*)$ satisfies*

$$\sqrt{n} \cdot \frac{\hat{f}^B(\mathbf{x}_*) - f_0(\mathbf{x}_*)}{\sqrt{r^2\xi_{1,r}(\mathbf{x}_*)}} \xrightarrow{d} \mathcal{N}(0, 1).$$

Theorem 3.7 establishes the asymptotic normality of the ensembled predictor \hat{f}^B for any fixed $\mathbf{x}_* \in \mathcal{A}_{\delta_n}$. For valid inference, it is essential that the bias vanishes asymptotically at each fixed point \mathbf{x}_* . However, in Corollary 3.6, the vanishing of the bias is established in the L_2 sense with respect to the random covariate $\mathbf{X} \in \mathcal{X}$, which does not imply almost sure convergence with respect to \mathbf{X} . To bridge this gap, additional analysis is required to identify a sufficiently large subset of the covariate space, on which the desired asymptotic normality holds, and whose probability measure tends to one as $n \rightarrow \infty$. As a result, the inference result holds with high probability for almost all $\mathbf{x} \in \mathcal{X}$. Finally, as the analytic form of $\xi_{1,r}(\mathbf{x}_*)$ is unavailable, the following theorem provides a consistent estimator of it.

Theorem 3.8. *Under the same setting as in Theorem 3.7, and recall the definition of $\hat{\sigma}_*^2$ in (2.9), it holds that for fixed $\mathbf{x}_* \in \mathcal{X}$,*

$$\sqrt{\frac{r^2\xi_{1,r}(\mathbf{x}_*)}{n\hat{\sigma}_*^2}} \xrightarrow{p} 1.$$

For the confidence interval in (2.7), Theorem 3.8 and the Slutsky theorem ensure that, as $n \rightarrow \infty$, it holds that

$$\mathbb{P}\left(\mathbb{E}(y_*|\mathbf{x}_*) \in [\hat{L}(\mathbf{x}_*), \hat{U}(\mathbf{x}_*)]\right) \rightarrow 1 - \alpha,$$

where

$$\hat{L}(\mathbf{x}_*) = \psi'\left(\hat{f}^B(\mathbf{x}_*) - z_{1-\alpha/2}\hat{\sigma}_*\right), \quad \hat{U}(\mathbf{x}_*) = \psi'\left(\hat{f}^B(\mathbf{x}_*) + z_{1-\alpha/2}\hat{\sigma}_*\right).$$

Here, $z_{1-\alpha/2}$ is the $(1 - \alpha/2)$ -th quantile of the standard normal distribution.

4 Numerical Experiments

We conduct numerical experiments under three generalized nonparametric regression models, i.e., logistic, Poisson and Binomial, to: [Aim (i)] assess the performance of our ensemble subsampling method (ESM) in terms of point estimate, estimated variance $\hat{\sigma}_*$, coverage probability, and average confidence interval length; [Aim (ii)] investigate the performance with different non-linear forms of g ; [Aim (iii)] examine the effect of the input dimension p ; [Aim (iv)] check the performance with different structures of neural networks. We first define the truth of $g(\mathbf{x})$ as

$$g(\mathbf{x}) = -x_1 + x_2 + x_3 \cdot x_4 + \frac{2}{1 + |x_5|}.$$

Here, x_j is the j -th element in the vector \mathbf{x} . We independently generate \mathbf{x}_i from $\mathcal{N}(0, \mathbf{I}_p)$ with $p = 10$, i.e., the first 5 covariates are signals and the rest are noise variables. We simulate n samples $\{\mathbf{x}_i, y_i\}$ for each model as follows.

Logistic Regression: The probability of y_i is given by

$$\mathbb{P}(y_i = 1|\mathbf{x}_i) = \frac{1}{1 + \exp\{-g(\mathbf{x}_i)\}}, \quad \mathbb{P}(y_i = 0|\mathbf{x}_i) = \frac{1}{1 + \exp\{g(\mathbf{x}_i)\}}.$$

In this model, we have $f_0(\mathbf{x}) = g(\mathbf{x})$ and $\psi'(x) = (1 + \exp(-x))^{-1}$.

Poisson Model: The probability mass of y_i given \mathbf{x}_i is

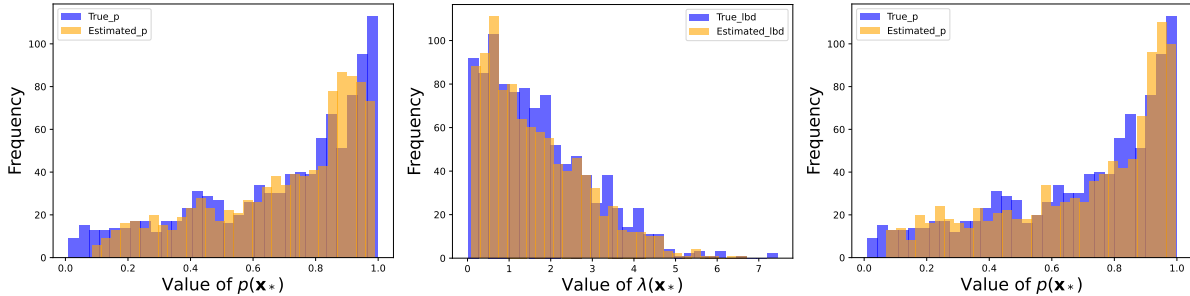
$$\mathbb{P}(y_i = k|\mathbf{x}_i) = \frac{e^{-\lambda(\mathbf{x}_i)} (\lambda(\mathbf{x}_i))^k}{k!},$$

where we set $\lambda(\mathbf{x}_i) = \log(1 + e^{g(\mathbf{x}_i)})$ to ensure that $\lambda(\mathbf{x}_i) > 0$ and prevent $\lambda(\mathbf{x}_i)$ from becoming excessively large, resulting in unreasonably large y_i . In this model, we have $f_0(\mathbf{x}_i) = \log\{\lambda(\mathbf{x}_i)\}$ and $\psi'(x) = \exp(x)$.

Binomial model: With $k \in \{0, 1, \dots, n_{\text{trial}}\}$, the probability mass of y_i is given by

$$\mathbb{P}(y_i = k|\mathbf{x}_i) = \binom{n_{\text{trial}}}{k} p^k (\mathbf{x}^{(i)}) (1 - p(\mathbf{x}^{(i)}))^k, \quad p(\mathbf{x}^{(i)}) = \frac{1}{1 + \exp\{-g(\mathbf{x}_i)\}}.$$

Under this model, $f_0(\mathbf{x}) = g(\mathbf{x})$ and $\psi'(x) = n_{\text{trial}}(1 + \exp(-x))^{-1}$.



(a) Histogram in logistic models (b) Histogram in Poisson models (c) Histogram in Binomial models

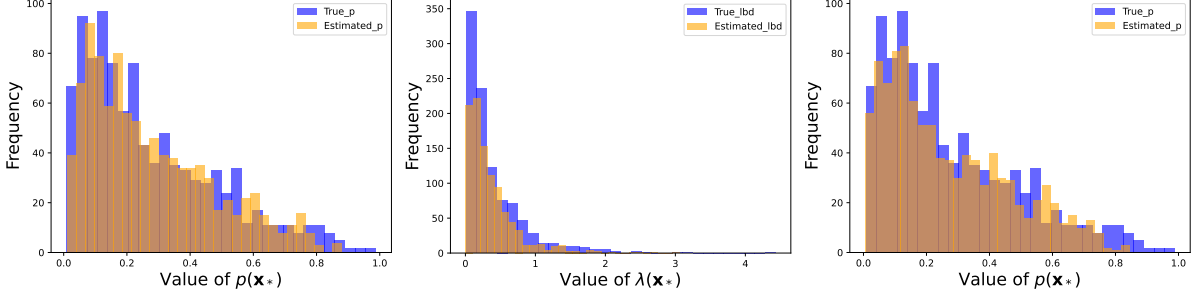
Figure 1: Histograms of $\psi'(\hat{f}^B(x_{\text{test}}))$ and $\psi'(f_0(x_{\text{test}}))$. Results are shown for (1a) logistic model, (1b) Poisson model and (1c) Binomial model with $n = 700$ and subsampling ratio $r = n^{0.9}$.

Table 1: Simulation results for different regressions under varying sample sizes n and subsampling ratios r . Key metrics include prediction bias (Bias_f , $\text{Bias}_{\psi'}$), mean absolute error (MAE_f , $\text{MAE}_{\psi'}$), empirical standard deviation (EmpSD), estimated standard error (SE), coverage probability (CP), and interval length (AIL). We set $\alpha = 0.05$.

	Bias_f	MAE_f	$\text{Bias}_{\psi'}$	$\text{MAE}_{\psi'}$	EmpSD	SE	CP	AIL
Logistic Model								
$n = 400, r = n^{0.8}$	0.34	0.80(0.69)	0.04	0.11(0.12)	1.06	0.94	93.2%	0.44(0.23)
$r = n^{0.85}$	0.14	0.71(0.63)	0.03	0.10(0.11)	0.95	0.87	93.9%	0.44(0.21)
$r = n^{0.9}$	-0.01	0.68(0.61)	0.01	0.10(0.10)	0.91	0.79	91.9%	0.43(0.18)
Bootstrap with f_0	-0.15	0.87(0.72)	-0.02	0.12(0.12)	1.13	-	96.0%	0.64(0.21)
$n = 700, r = n^{0.8}$	0.34	0.74(0.63)	0.04	0.10(0.10)	0.97	0.95	95.3%	0.45(0.23)
$r = n^{0.85}$	0.12	0.66(0.57)	0.03	0.09(0.10)	0.87	0.86	94.6%	0.44(0.21)
$r = n^{0.9}$	-0.02	0.66(0.57)	0.01	0.09(0.09)	0.87	0.79	92.4%	0.43(0.19)
Bootstrap with f_0	-0.31	0.88(0.73)	-0.03	0.12(0.11)	1.15	-	96.6%	0.73(0.16)
Poisson Model								
$n = 400, r = n^{0.8}$	-0.27	0.38(0.35)	-0.32	0.43(0.44)	0.52	0.43	92.9%	1.86(1.14)
$r = n^{0.85}$	-0.20	0.34(0.33)	-0.24	0.40(0.41)	0.48	0.43	94.8%	2.08(1.31)
$r = n^{0.9}$	-0.13	0.32(0.31)	-0.16	0.39(0.40)	0.45	0.45	96.2%	2.30(1.45)
Bootstrap with f_0	-0.08	0.46(0.41)	-0.01	0.63(0.65)	0.62	-	92.4%	4.46(3.77)
$n = 700, r = n^{0.8}$	-0.10	0.29(0.30)	-0.20	0.37(0.38)	0.42	0.38	94.3%	1.79(0.95)
$r = n^{0.85}$	-0.06	0.28(0.29)	-0.15	0.35(0.36)	0.40	0.38	95.8%	1.92(1.02)
$r = n^{0.9}$	0.02	0.27(0.29)	-0.06	0.33(0.34)	0.40	0.39	97.2%	2.18(1.22)
Bootstrap with f_0	-0.02	0.41(0.38)	-0.11	0.55(0.56)	0.56	-	95.0%	4.16(3.10)
Binomial Model								
$n = 400, r = n^{0.8}$	0.42	0.65(0.57)	0.04	0.08(0.09)	0.86	0.64	87.6%	0.30(0.00)
$r = n^{0.85}$	0.32	0.58(0.51)	0.03	0.07(0.08)	0.77	0.66	91.3%	0.31(0.00)
$r = n^{0.9}$	0.24	0.53(0.45)	0.03	0.07(0.07)	0.70	0.68	94.7%	0.33(0.00)
Bootstrap with f_0	0.25	0.72(0.61)	0.02	0.09(0.10)	0.94	-	95.5%	0.48(0.24)
$n = 700, r = n^{0.8}$	0.24	0.45(0.39)	0.03	0.06(0.06)	0.59	0.55	94.3%	0.27(0.01)
$r = n^{0.85}$	0.15	0.41(0.35)	0.02	0.05(0.05)	0.54	0.56	96.0%	0.28(0.01)
$r = n^{0.9}$	0.09	0.39(0.33)	0.02	0.05(0.05)	0.51	0.57	97.3%	0.30(0.01)
Bootstrap with f_0	0.09	0.60(0.46)	0.00	0.08(0.08)	0.76	-	94.9%	0.39(0.20)

For Aim (i), we randomly select sub-datasets of size r to train neural networks, varying r from $n^{0.8}$ to $n^{0.9}$, with $n = 400$ and 700 . Based on our experiments, we recommend $r = n^{0.9}$, balancing two key factors: (1) a sufficiently large r ensures neural network convergence and strong performance by providing ample training data, and (2) r remains smaller than the total sample size n . To maintain computational feasibility, we set the number of subsampling iterations to $B = 1400$. The testing data, generated similarly to the training data, has a size of $n_{\text{test}} = 1000$. We apply the DNN-based ESM algorithm with a network structure of $L = 3$ and $\mathbf{p} = (p, 128, 64, 1)$. Each hidden layer incorporates a 10% dropout rate for regularization, and we apply ℓ_2 regularization with a weight decay rate of 0.02. The learning rate is fine-tuned for optimal validation convergence. To keep network outputs within a reasonable range, we implement early stopping with a maximum of 500 epochs to prevent overfitting. The activation function used is ReLU.

With $\hat{f}^B(\cdot)$ being the output of our algorithm, we evaluate its performance using n_{test} test



(a) Histogram in logistic models (b) Histogram in Poisson models (c) Histogram in Binomial models

Figure 2: Histograms of $\psi'(\hat{f}^B(x_{\text{test}}))$ and $\psi'(f_0(x_{\text{test}}))$. Results are shown for **2a** logistic model, **2b** Poisson model (count outcomes) and **2c** Binomial model (count outcomes) with $n = 700$ and subsampling ratio $r = n^{0.9}$.

points across the following metrics.

- Bias_f : the average bias between \hat{f}^B and f_0 .
- MAE_f : the mean absolute error between \hat{f}^B and f_0 .
- $\text{Bias}_{\psi'}$: the average bias in the transformed form $\psi'(\hat{f}^B)$ and $\psi'(f_0)$.
- $\text{MAE}_{\psi'}$: the mean absolute error between $\psi'(\hat{f}^B)$ and $\psi'(f_0)$.
- EmpSD : the empirical standard deviation of \hat{f}^B , given by
$$\left(\frac{1}{n_{\text{test}}} \sum_{i=1}^{n_{\text{test}}} (\hat{f}^B(\mathbf{x}_{\text{test},i}) - f_0(\mathbf{x}_{\text{test},i}))^2 \right)^{\frac{1}{2}}.$$
- SE : the square root of the average estimated variance $\hat{\sigma}_*^2$.
- CP (Coverage Probability): the proportion of times the inference interval covers the true value $\psi'(f_0(\mathbf{x}_{\text{test},i}))$ for $i \in [n_{\text{test}}]$.
- AIL (Average Interval Length): $\frac{1}{n_{\text{test}}} \sum_{i=1}^{n_{\text{test}}} (U_i - L_i)$, where U_i and L_i are the upper and lower bounds of the prediction interval for test instance $\mathbf{x}_{\text{test},i}$.

Numbers in brackets reported in the tables represent the standard deviation of each metric across test data points.

Table 1 presents the results of our method across logistic, Poisson, and Binomial models. Increasing the sample size n reduces prediction deviations, as reflected in decreasing mean absolute errors (MAE) for both f and its transformed counterpart ψ' . The close alignment between empirical standard deviations (EmpSD) and estimated standard errors (SE) confirms the accuracy of SE. Our method consistently achieves coverage probabilities (CP) near the 95% target. Additionally, the average interval lengths (AIL) are substantially shorter than those from bootstrap intervals, suggesting its efficiency in uncertainty estimation. In the bootstrap approach with unknown f_0 , we estimate \hat{f} from one data half and evaluate the distribution of $f_0 - \hat{f}$ on the other half to determine the 95 percentile. While bootstrap with f_0 achieves nominal coverage (95%), its wider intervals indicate conservative uncertainty estimates. Figure 1 supports our findings and show that $\psi'(\hat{f}^B(\mathbf{x}_{\text{test}}))$ aligns well with $\psi'(f_0(\mathbf{x}_{\text{test}}))$. Despite the wide range of true values, our confidence intervals remain tight, with AILs as low as 0.43–0.45 for logistic models and 1.86–2.3 for Poisson models, indicating the precision of ESM in uncertainty quantification.

Table 2: Simulation results for different models under varying sample sizes n and subsampling ratios r with non-linear function g_1 .

	Bias _{f}	MAE _{f}	Bias _{ψ'}	MAE _{ψ'}	EmpSD	SE	CP	AIL
Logistic Model								
$n = 400, r = n^{0.8}$	-0.70	0.99(0.83)	-0.08	0.13(0.13)	1.29	1.19	91.3%	0.52(0.26)
$r = n^{0.85}$	-0.40	0.83(0.69)	-0.05	0.12(0.12)	1.09	1.11	95.1%	0.54(0.23)
$r = n^{0.9}$	-0.15	0.72(0.60)	-0.02	0.12(0.11)	0.94	0.96	95.1%	0.52(0.20)
Bootstrap with f_0	-0.22	1.15(1.04)	-0.00	0.16(0.14)	1.55	-	95.4%	0.76(0.23)
$n = 700, r = n^{0.8}$	-0.34	0.75(0.67)	-0.04	0.11(0.12)	1.01	0.96	93.3%	0.47(0.22)
$r = n^{0.85}$	-0.11	0.65(0.58)	-0.02	0.10(0.11)	0.87	0.86	94.3%	0.46(0.20)
$r = n^{0.9}$	0.05	0.61(0.54)	0.00	0.10(0.10)	0.81	0.76	93.2%	0.44(0.17)
Bootstrap with f_0	0.08	0.76(0.63)	-0.01	0.12(0.11)	0.99	-	95.9%	0.63(0.12)
Poisson Model								
$n = 400, r = n^{0.8}$	-0.69	0.75(0.59)	-0.19	0.21(0.33)	0.95	0.70	85.6%	0.63(0.60)
$r = n^{0.85}$	-0.46	0.59(0.51)	-0.15	0.19(0.31)	0.78	0.70	93.3%	0.78(0.75)
$r = n^{0.9}$	-0.27	0.51(0.44)	-0.11	0.18(0.30)	0.67	0.69	95.6%	0.94(0.93)
Bootstrap with f_0	-0.19	0.72(0.59)	-0.07	0.25(0.36)	0.93	-	94.3%	2.25(2.39)
$n = 700, r = n^{0.8}$	-0.40	0.59(0.50)	-0.14	0.19(0.31)	0.78	0.67	93.8%	0.75(0.68)
$r = n^{0.85}$	-0.17	0.50(0.42)	-0.09	0.18(0.29)	0.66	0.67	97.0%	0.93(0.88)
$r = n^{0.9}$	0.01	0.47(0.39)	-0.04	0.17(0.27)	0.61	0.65	95.9%	1.07(1.05)
Bootstrap with f_0	0.04	0.70(0.56)	-0.01	0.25(0.34)	0.90	-	96.1%	2.49(2.61)
Binomial Model								
$n = 400, r = n^{0.8}$	-0.21	0.58(0.54)	-0.03	0.09(0.10)	0.79	0.60	89.7%	0.33(0.01)
$r = n^{0.85}$	-0.14	0.57(0.51)	-0.02	0.09(0.10)	0.76	0.62	91.1%	0.35(0.02)
$r = n^{0.9}$	-0.08	0.56(0.49)	-0.02	0.09(0.10)	0.75	0.63	91.1%	0.36(0.02)
Bootstrap with f_0	-0.28	0.90(0.76)	-0.02	0.13(0.13)	1.18	-	96.9%	0.69(0.22)
$n = 700, r = n^{0.8}$	-0.18	0.47(0.45)	-0.02	0.07(0.09)	0.66	0.54	91.1%	0.29(0.01)
$r = n^{0.85}$	-0.12	0.45(0.43)	-0.02	0.07(0.08)	0.62	0.55	92.9%	0.30(0.02)
$r = n^{0.9}$	-0.06	0.44(0.42)	-0.01	0.07(0.08)	0.60	0.56	94.2%	0.32(0.02)
Bootstrap with f_0	-0.03	0.60(0.50)	-0.00	0.10(0.10)	0.78	-	95.0%	0.44(0.16)

For Aim (ii), we assess our method’s performance across different nonlinear forms of g in three regression frameworks. Unlike the basic settings, we modify g to examine how different nonlinear generative models impact estimation accuracy and to demonstrate ESM’s adaptability. Specifically, we define

$$g_1(\mathbf{x}) = x_1 + |x_2 x_3| - e^{0.2x_4} - \log(1 + 2|x_5|),$$

which introduces interactions, exponential decay, and logarithmic effects. Compared to g , g_1 skews logistic model probabilities toward 0 and also produces a narrower range for Poisson model parameters λ .

Table 2 shows that results under g_1 remain consistent with previous findings. Increasing sample size decreases MAE for $\psi'(\hat{f}^B)$ and \hat{f}^B . Empirical standard deviations (empSD) and estimated standard errors (SE) remain well aligned, with coverage probabilities maintaining 95% validity. ESM also achieves narrower confidence intervals without sacrificing coverage accuracy compared to bootstrap intervals. Figure 2 illustrates histograms of true versus estimated transformed predictions

Table 3: Simulation results for different models under varying sample sizes n and subsampling ratios r with $p = 100$.

	Bias _{f}	MAE _{f}	Bias _{ψ'}	MAE _{ψ'}	EmpSD	SE	CP	AIL
Logistic Model								
$n = 400, r = n^{0.8}$	0.29	1.22(0.98)	0.05	0.18(0.17)	1.57	1.26	89.0%	0.63(0.23)
$r = n^{0.85}$	0.44	1.32(1.04)	0.06	0.18(0.17)	1.68	1.52	92.0%	0.68(0.25)
$r = n^{0.9}$	0.55	1.45(1.12)	0.05	0.19(0.18)	1.83	1.82	94.6%	0.72(0.27)
Bootstrap with f_0	0.72	2.05(1.52)	0.04	0.25(0.21)	2.55	-	96.2%	0.86(0.20)
$n = 700, r = n^{0.8}$	0.28	1.12(0.93)	0.05	0.16(0.16)	1.45	1.36	93.8%	0.65(0.24)
$r = n^{0.85}$	0.39	1.20(0.98)	0.05	0.17(0.16)	1.54	1.55	95.0%	0.68(0.25)
$r = n^{0.9}$	0.45	1.27(1.02)	0.05	0.17(0.16)	1.63	1.75	96.0%	0.72(0.26)
Bootstrap with f_0	0.80	1.85(1.38)	0.06	0.21(0.19)	2.31	-	97.3%	0.85(0.21)
Poisson Model								
$n = 400, r = n^{0.8}$	-0.66	0.88(0.57)	-0.90	0.99(0.89)	1.05	0.72	84.5%	2.38(0.97)
	-0.67	0.89(0.60)	-0.85	0.96(0.86)	1.07	0.85	92.1%	3.16(1.41)
	-0.64	0.87(0.63)	-0.77	0.91(0.83)	1.08	0.97	95.5%	4.26(2.06)
Bootstrap with f_0	-0.60	1.07(0.90)	-0.52	1.05(0.96)	1.40	-	95.5%	21.9(22.2)
$n = 700, r = n^{0.8}$	-0.67	0.89(0.63)	-0.81	0.93(0.82)	1.09	0.75	87.2%	2.50(1.07)
$r = n^{0.85}$	-0.61	0.86(0.65)	-0.72	0.88(0.78)	1.08	0.83	91.4%	3.19(1.43)
$r = n^{0.9}$	-0.52	0.82(0.65)	-0.61	0.84(0.74)	1.05	0.92	94.0%	4.11(1.93)
Bootstrap with f_0	-0.50	0.94(0.85)	-0.44	0.92(0.84)	1.27	-	96.2%	19.9(18.9)
Binomial Model								
$n = 400, r = n^{0.8}$	0.49	1.19(0.99)	0.07	0.17(0.16)	1.55	1.01	81.9%	0.49(0.01)
$r = n^{0.85}$	0.55	1.27(1.06)	0.06	0.17(0.16)	1.65	1.20	86.0%	0.54(0.01)
$r = n^{0.9}$	0.58	1.37(1.13)	0.05	0.17(0.16)	1.78	1.39	88.6%	0.59(0.00)
Bootstrap with f_0	0.31	1.39(1.08)	0.02	0.18(0.17)	1.76	-	95.9%	0.77(0.24)
$n = 700, r = n^{0.8}$	0.68	1.12(0.95)	0.09	0.15(0.15)	1.47	1.11	88.1%	0.50(0.00)
$r = n^{0.85}$	0.69	1.16(0.98)	0.08	0.14(0.14)	1.52	1.25	90.8%	0.54(0.00)
$r = n^{0.9}$	0.68	1.18(1.01)	0.07	0.14(0.14)	1.55	1.39	93.4%	0.59(0.01)
Bootstrap with f_0	0.51	1.33(1.05)	0.06	0.17(0.16)	1.69	-	96.5%	0.76(0.23)

for $g_1(\mathbf{x})$. Unlike Figure 1, where predictions skew toward 1, the logistic model’s $p(\mathbf{x})$ under g_1 shifts leftward toward 0. In the Poisson model, $\lambda(\mathbf{x})$ spans a narrower range than under $g(\mathbf{x})$, demonstrating ESM’s robustness across these two nonlinear settings.

For Aim (iii), we increase the number of input dimensions while retaining only a few elements that are relevant to the true output logits f_0 . As the dimensionality grows, the data signals become increasingly obscured within the larger feature space, making it harder for neural networks to accurately capture these signal features. This results in a significant deviation between the estimated $\mathbb{E}(y|\mathbf{x})$ and the true $\mathbb{E}(y|\mathbf{x})$, which can also lead to inflated overall interval lengths. Table 3 shows that MAE _{f} , MAE _{ψ'} , and AIL are notably larger compared to those in Table 1. Despite these challenges, the inference framework remains remarkably robust. The coverage probability (CP) stays stable at around 95% in most cases, even under large deviations, except when the subsample size r is relatively small.

Aim (iv) investigates whether narrower yet deeper architectures can maintain robust performance under our Ensemble Subsampling Method (ESM). To explore this, we design a deeper

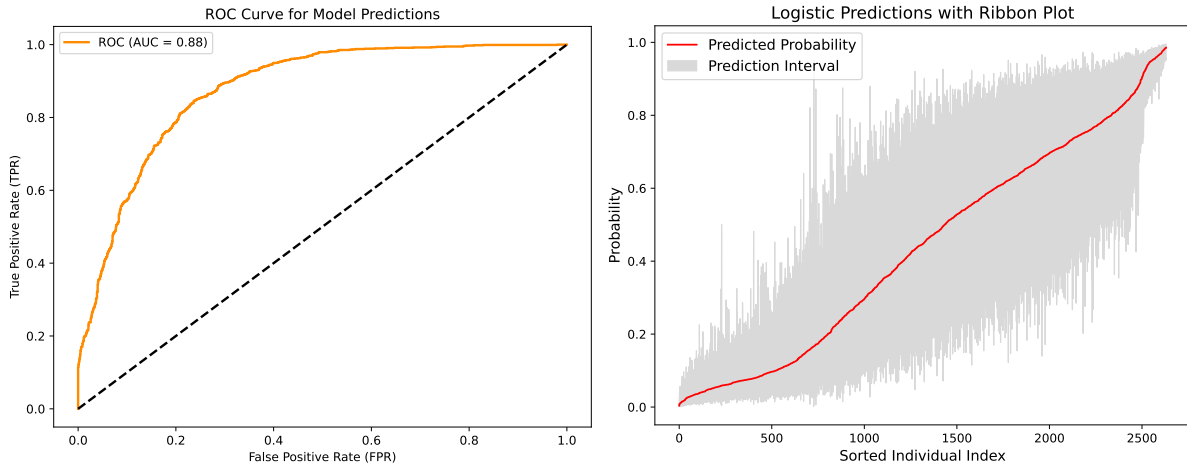
Table 4: Simulation results for different models under varying sample sizes n and subsampling ratios r with a deeper neural network.

	Bias _{f}	MAE _{f}	Bias _{ψ'}	MAE _{ψ'}	EmpSD	SE	CP	AIL
Logistic Model								
$n = 400, r = n^{0.8}$	-0.03	0.75(0.66)	0.01	0.11(0.12)	1.00	1.03	94.4%	0.53(0.25)
$r = n^{0.85}$	-0.05	0.74(0.65)	0.01	0.11(0.11)	0.99	1.11	95.9%	0.57(0.25)
$r = n^{0.9}$	-0.09	0.74(0.64)	0.01	0.10(0.11)	0.98	1.21	97.8%	0.62(0.23)
Bootstrap with f_0	-0.08	1.56(1.17)	-0.02	0.22(0.21)	1.94	-	96.7%	0.79(0.13)
$n = 700, r = n^{0.8}$	0.07	0.71(0.61)	0.04	0.10(0.10)	0.94	0.97	94.5%	0.51(0.24)
$r = n^{0.85}$	0.02	0.72(0.62)	0.03	0.10(0.10)	0.94	1.04	95.9%	0.55(0.23)
$r = n^{0.9}$	-0.05	0.73(0.62)	0.02	0.10(0.09)	0.95	1.16	97.1%	0.61(0.22)
Bootstrap with f_0	-0.06	1.61(1.15)	-0.01	0.23(0.21)	1.98	-	94.6%	0.77(0.14)
Poisson Model								
$n = 400, r = n^{0.8}$	-0.13	0.34(0.34)	-0.33	0.45(0.52)	0.48	0.42	93.5%	1.82(0.75)
$r = n^{0.85}$	-0.07	0.32(0.33)	-0.26	0.42(0.48)	0.46	0.44	95.8%	2.09(0.87)
$r = n^{0.9}$	-0.02	0.31(0.33)	-0.20	0.39(0.44)	0.46	0.49	98.1%	2.50(1.08)
Bootstrap with f_0	-0.20	0.76(0.80)	0.05	0.82(0.77)	1.10	-	95.1%	19.9(15.8)
$n = 700, r = n^{0.8}$	-0.06	0.33(0.34)	-0.29	0.43(0.49)	0.47	0.39	92.8%	1.83(0.78)
$r = n^{0.85}$	-0.01	0.31(0.34)	-0.22	0.40(0.45)	0.46	0.41	95.3%	2.07(0.91)
$r = n^{0.9}$	0.04	0.30(0.34)	-0.16	0.37(0.41)	0.46	0.45	97.3%	2.44(1.13)
Bootstrap with f_0	-0.24	0.70(0.70)	-0.19	0.75(0.76)	0.99	-	94.7%	12.9(10.5)
Binomial Model								
$n = 400, r = n^{0.8}$	0.29	0.63(0.59)	0.05	0.09(0.10)	0.86	0.60	86.5%	0.31(0.01)
$r = n^{0.85}$	0.23	0.60(0.56)	0.05	0.08(0.09)	0.82	0.64	89.2%	0.33(0.03)
$r = n^{0.9}$	0.19	0.57(0.52)	0.04	0.08(0.09)	0.77	0.71	93.0%	0.37(0.06)
Bootstrap with f_0	0.72	1.17(0.97)	0.06	0.13(0.12)	1.52	-	92.2%	0.55(0.28)
$n = 700, r = n^{0.8}$	0.07	0.49(0.45)	0.03	0.06(0.06)	0.67	0.55	92.5%	0.30(0.05)
$r = n^{0.85}$	0.03	0.48(0.44)	0.02	0.06(0.06)	0.65	0.60	94.4%	0.33(0.06)
$r = n^{0.9}$	-0.01	0.47(0.44)	0.02	0.06(0.05)	0.65	0.68	96.2%	0.38(0.09)
Bootstrap with f_0	0.13	0.97(0.84)	-0.01	0.11(0.11)	1.28	-	94.8%	0.61(0.27)

network with $L = 5$ and the layer structure $\mathbf{p} = (p, 10, 15, 20, 25, 1)$. It is well known that training deep networks poses the risk of gradient explosion or vanishing during backpropagation (Glorot and Bengio, 2010). To improve training stability, we incorporate batch normalization layers after the second and second-to-last layers. These modifications aim to mitigate gradient instability while maintaining the network’s ability to learn complex representations under the ESM framework. Table 4 shows the performance of deeper, narrower neural networks. Despite the increased depth, prediction deviations remain small and comparable to those of shallow, wide networks. Key metrics, including empSD, SE and CP, align well with theoretical expectations, indicating robust inferential validity. However, AIL for deeper networks is somewhat wider than that in the baseline setting, as additional layers introduce non-linear interactions that may amplify variability in uncertainty estimates.

5 Analysis of eICU data

Predicting ICU readmission is vital for improving patient outcomes and reducing healthcare costs. Readmitted patients face higher mortality risks and increased expenses, while hospitals must optimize resource use. Identifying high-risk individuals allows for more personalized care, such as closer monitoring. The eICU Collaborative Research Database (eICU-CRD) (Pollard et al., 2018) is a large-scale, multi-center collection of anonymized ICU patient data, created through collaboration between the MIT Laboratory for Computational Physiology and healthcare organizations. It includes detailed information on patients’ physiological measurements, clinical data, lab results, medication usage, and outcomes during their ICU stays. Our analysis focuses on Hospital #188, a major hospital with 2,632 patients admitted to ICU. We focus on 20 laboratory results, including chloride, white blood cell (WBC) count, hemoglobin (Hgb), red cell distribution width (RDW), calcium, platelet count, mean corpuscular volume (MCV), and mean corpuscular hemoglobin concentration (MCHC), which have been identified in the medical literature as predictors of hospitalization. Combined with other patient demographic information, this results in a total of 55 covariates for analysis. Regarding outcomes, among the 2,632 patients admitted to the ICU, 1,476 were not readmitted, 1,046 were readmitted once, 77 were readmitted twice, 26 were readmitted three times, and 7 were readmitted five or more times. We apply nonparametric logistic and Poisson models to, respectively, predict ICU readmission and the total number of ICU readmissions using our ESM. To evaluate the effectiveness of our methods, we perform 5-fold cross-validation. Specifically, we divide the data into five equal-sized subsamples, train the model on four subsamples, and use the ESM method to estimate the mean and corresponding inference interval for the held-out fold. This process is repeated across all five folds, allowing us to obtain point estimates and intervals for all sample points.



(a) ROC curve in the nonparametric logistic model

(b) Individual intervals in logistic Model

Figure 3: Evaluation in the logistic model. Figure 3a presents the ROC curve for the logistic model, illustrating the model’s ability to estimate prediction mean, with an AUC of 0.86. Figure 3b displays individual estimates along with their corresponding confidence intervals, highlighting the heteroskedasticity observed across individuals.

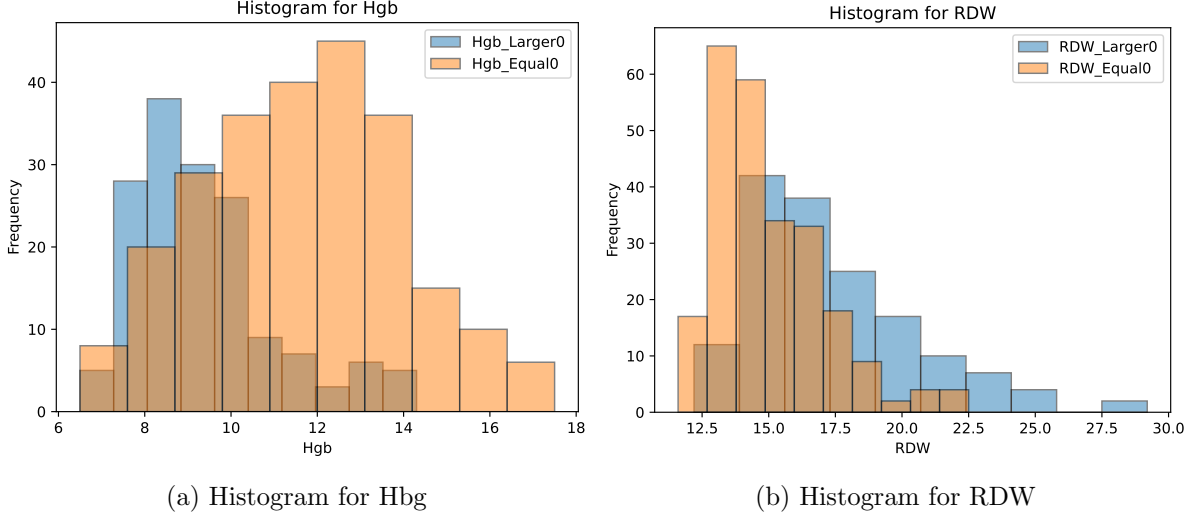


Figure 4: Histogram under distinct probability intervals in logistic models. Figures 4a and 4b present hemoglobin (Hgb) and red cell distribution width (RDW) under different probability intervals. The blue histograms represent patients for whom the whole probability interval is above 0.7, whereas the orange histograms represent patients for whom the whole probability interval is below 0.15.

For predicting ICU readmission, we define the binary outcome as: $y = 0$ for readmission times of zero, and $y = 1$ for readmission times greater than or equal to one. A high probability of $y = 1$ predicted based on covariates suggests a high likelihood of ICU readmission for a given patient profile, indicating the need for more personalized care for these patients. To implement our method, we set the subsampling size to $r = n^{0.9} = 765$ and the number of subsampling iterations to $B = 3000$. The neural network used has the structure (55, 128, 64, 1) with the ReLU activation function. During training, we fine-tune the learning rate to $\eta = 0.2$, use 500 training epochs, and set the weight decay parameter to 0.03.

As reported in Figure 3a, the Area under the Receiver Operating Characteristic Curve (AUC-ROC) is around 0.86, showing a satisfactory performance of using DNN-estimated $\mathbb{E}(y|\mathbf{x})$ to distinguish patients. Further, Figure 3b shows the estimated probabilities and their corresponding confidence intervals across individuals. The x -axis represents individual cases (sorted by estimated probability for clarity), and the y -axis shows the estimated probability. The gray intervals indicate uncertainty, constructed using a significance level of $\alpha = 0.05$. Notably, both the estimated probabilities and interval lengths vary across individuals, reflecting heteroskedasticity in the model’s predictions. Even among individuals with similar predicted probabilities, uncertainty can differ, suggesting differences in data quality or individual characteristics that make some patients inherently more or less predictable.

Moreover, some interesting observations are available. Figure 4a shows patients with probability interval above 0.7 of ICU readmission exhibit significantly lower hemoglobin levels compared to those with probability interval below 0.3. Since hemoglobin is critical for oxygen transport, reduced levels may reflect compromised tissue oxygenation, potentially exacerbating organ dysfunction and increasing the likelihood of clinical deterioration that necessitates readmission. Additionally, Figure 4b shows that higher RDW (red cell distribution width) is also observed among patients with ICU readmission. Higher RDW is often associated with systemic inflammation, nutritional deficiency,

cies or impaired red blood cell production, all of which could signal unresolved physiologic stress or comorbidities that delay recovery and predispose patients to repeated critical care interventions, which may be factors that could contribute to the increased risk of ICU readmission. These findings align with previous studies (Vincent et al., 2002; Lippi and Plebani, 2014), further supporting the role of hematologic markers in predicting ICU readmission.

We also fit a nonparametric Poisson regression model by using DNN to estimate $\mathbb{E}(y|\mathbf{x}_*)$ for a new data point \mathbf{x}_* . The results may provide further insights into patient well-being with more detailed count data. Based on our numerical experience, we find that the same hyperparameters used in the nonparametric logistic regression model perform well in this case as well.

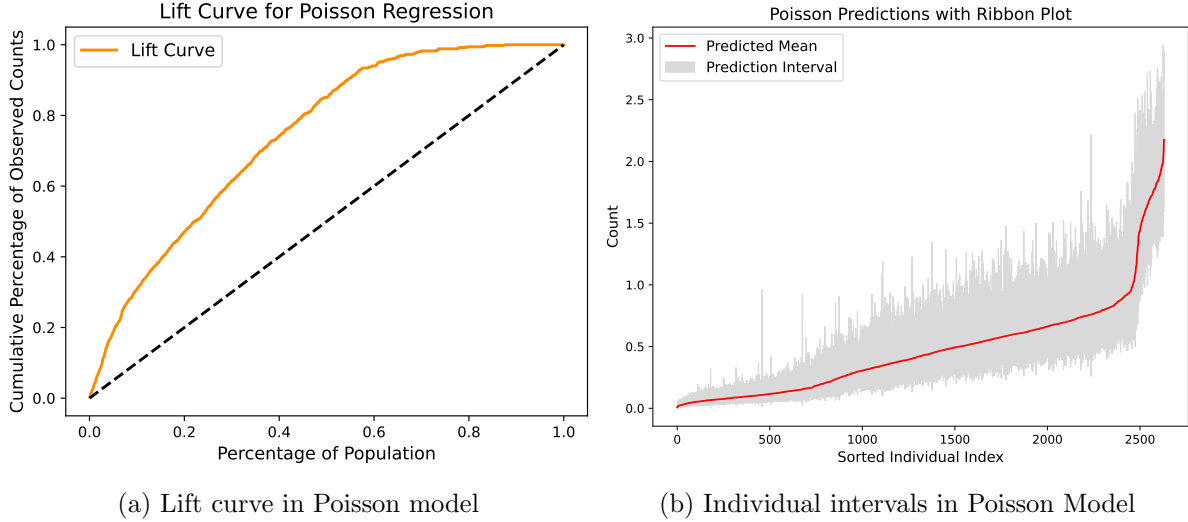


Figure 5: Evaluation in Poisson model. Figure 5a presents the lift curve for the Poisson model, illustrating the model’s ability to estimate prediction mean. Figure 5b shows individual estimates along with their corresponding confidence intervals.

Figure 5a presents the lift curve for the estimated nonparametric Poisson means, which evidently lies significantly above the random guess line, demonstrating the good accuracy of our estimate of $\mathbb{E}(y|\mathbf{x})$. Furthermore, the C-index for the Poisson model is 0.875, suggesting a decent discriminatory power. Figure 5b shows individual confidence intervals for the sorted $\hat{\lambda}(\mathbf{x}_*)$, the estimated subject-specific mean. The varying widths of the confidence intervals indicate heterogeneity in uncertainty, suggesting that the model captures individual-level differences in predictability. We observe differences in Hgb and RDW across distinct confidence intervals. When the estimated outcome intervals are low (i.e., the entire interval is below 0.1), the corresponding patients are more likely to have higher Hgb and lower RDW. In contrast, when the outcome intervals are high (with the lowest bound exceeding 0.5), these patients tend to have lower Hgb and higher RDW. These findings suggest that patients with low estimated readmissions exhibit anemia and increased red cell heterogeneity, whereas those with high estimated readmissions tend to have preserved hemoglobin and more uniform red blood cell size. The consistency of these associations across both nonparametric logistic and Poisson models highlights the robust predictive value of Hgb and RDW for the risk of ICU readmission.

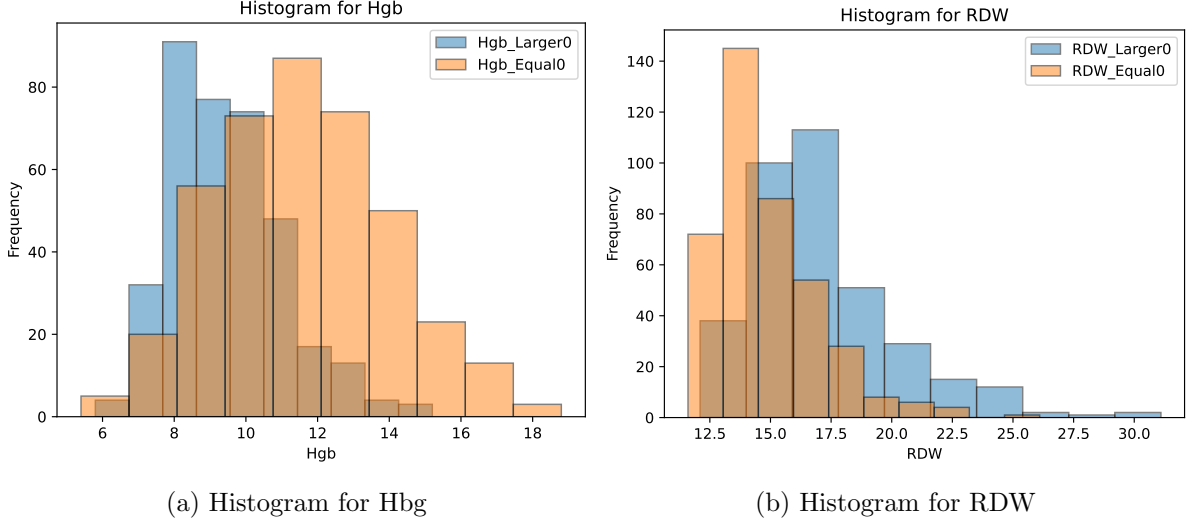


Figure 6: Histogram under distinct intervals in Poisson. Figures 6a and 6b present hemoglobi (Hgb) and red cell distribution width (RDW) under different intervals. The blue histograms represent patients for whom the whole probability interval is above 0.5, whereas the orange histograms represent patients for whom the whole probability interval is below 0.2.

6 Discussion

This paper focuses on drawing inference on estimated means for categorical outcomes or those belonging to the exponential family of distributions using deep neural networks (DNNs). Our approach is general, as we cast the problem within the generalized nonparametric regression model (GNRM) framework and develop a robust statistical approach for conducting inference on means estimated by DNNs. We address a critical gap in existing work by conducting the convergence rate analysis of DNNs in GNRM settings and integrating these results with the theoretical properties of U-statistics and Hoeffding decomposition. Building on this foundation, we introduce an ensemble subsampling method (ESM) to ensure valid prediction inference, specifically tailored for multi-layer neural networks under the GNRM framework. Through numerical experiments, we evaluate its finite-sample performance and demonstrate the practical utility of ESM with a detailed analysis of the eICU dataset, showing how our predictions and uncertainty measures can assist caregivers in providing more personalized care.

Our theoretical analysis centers on the ReLU activation function. For other activation functions, such as Leaky ReLU, monomial-based approximations of input elements remain feasible, although the associated approximation errors and convergence rates may vary. In contrast, sigmoid-like activations may require new theoretical frameworks and different regularization strategies due to their smoothness properties, which complicate achieving comparable approximations under bounded parameter constraints. Beyond extending our analysis to various activation functions, another interesting future direction is to explore how ESM can be extended to more complex data structures, such as time-series or spatial data. For instance, instead of focusing solely on iid data, future research could investigate how the ESM framework performs when applied to data with temporal dependencies, autocorrelation or spatial relationships. Developing prediction inference methods in such data set will extend the application of ESM in wider scenarios.

References

- ALAA, A. and VAN DER SCHAAR, M. (2020). Discriminative jackknife: Quantifying uncertainty in deep learning via higher-order influence functions. In *International Conference on Machine Learning*.
- ANGELOPOULOS, A. N. and BATES, S. (2021). A gentle introduction to conformal prediction and distribution-free uncertainty quantification. *arXiv preprint arXiv:2107.07511* .
- ATHEY, S., IMBENS, G. W. and WAGER, S. (2018). Approximate residual balancing: debiased inference of average treatment effects in high dimensions. *Journal of the Royal Statistical Society Series B: Statistical Methodology* **80** 597–623.
- BARBER, R. F., CANDÈS, E. J., RAMDAS, A. and TIBSHIRANI, R. J. (2021). Predictive inference with the jackknife+. *The Annals of Statistics* **49** 486–507.
- BARTLETT, P. L., LONG, P. M., LUGOSI, G. and TSIGLER, A. (2020). Benign overfitting in linear regression. *Proceedings of the National Academy of Sciences* **117** 30063–30070.
- BHATTACHARYA, S., FAN, J. and MUKHERJEE, D. (2024). Deep neural networks for nonparametric interaction models with diverging dimension. *The Annals of Statistics* **52** 2738–2766.
- BOROSIKH, Y. V. (2020). *U-statistics in Banach Spaces*. Walter de Gruyter GmbH & Co KG.
- DRUCKER, H., BURGESS, C. J., KAUFMAN, L., SMOLA, A. and VAPNIK, V. (1996). Support vector regression machines. *Advances in neural information processing systems* **9**.
- FAN, J. (2018). *Local polynomial modelling and its applications: monographs on statistics and applied probability* 66. Routledge.
- FAN, J. and GU, Y. (2024). Factor augmented sparse throughput deep relu neural networks for high dimensional regression. *Journal of the American Statistical Association* **119** 2680–2694.
- FAN, J., GU, Y. and ZHOU, W.-X. (2024). How do noise tails impact on deep relu networks? *The Annals of Statistics* **52** 1845–1871.
- FEI, Z. and LI, Y. (2021). Estimation and inference for high dimensional generalized linear models: A splitting and smoothing approach. *Journal of Machine Learning Research* **22** 1–32.
- FEI, Z. and LI, Y. (2024). U-learning for prediction inference via combinatorial multi-subsampling: With applications to lasso and neural networks. *arXiv preprint arXiv:2407.15301* .
- FREES, E. W. (1989). Infinite order u-statistics. *Scandinavian Journal of Statistics* 29–45.
- GLOROT, X. and BENGIO, Y. (2010). Understanding the difficulty of training deep feedforward neural networks. In *Proceedings of the thirteenth international conference on artificial intelligence and statistics*. JMLR Workshop and Conference Proceedings.
- GUO, Z., RAKSHIT, P., HERMAN, D. S. and CHEN, J. (2021). Inference for the case probability in high-dimensional logistic regression. *Journal of Machine Learning Research* **22** 1–54.

- GYÖRFI, L., KOHLER, M., KRZYŻAK, A. and WALK, H. (2006). *A distribution-free theory of nonparametric regression*. Springer Science & Business Media.
- HASTIE, T., TIBSHIRANI, R., FRIEDMAN, J. H. and FRIEDMAN, J. H. (2009). *The Elements of Statistical Learning: Data mining, Inference, and Prediction*. Springer.
- HOEFFDING, W. (1992). A class of statistics with asymptotically normal distribution. *Breakthroughs in statistics: Foundations and basic theory* 308–334.
- HORNIK, K., STINCHCOMBE, M. and WHITE, H. (1989). Multilayer feedforward networks are universal approximators. *Neural networks* **2** 359–366.
- HUANG, J., XI, H., ZHANG, L., YAO, H., QIU, Y. and WEI, H. (2024). Conformal prediction for deep classifier via label ranking. In *International Conference on Machine Learning*.
- JIAO, Y., SHEN, G., LIN, Y. and HUANG, J. (2023). Deep nonparametric regression on approximate manifolds: Nonasymptotic error bounds with polynomial prefactors. *The Annals of Statistics* **51** 691–716.
- KIM, B., XU, C. and BARBER, R. (2020). Predictive inference is free with the jackknife+-after-bootstrap. *Advances in Neural Information Processing Systems* **33** 4138–4149.
- KOHLER, M. and KRZYŻAK, A. (2005). Adaptive regression estimation with multilayer feedforward neural networks. *Nonparametric Statistics* **17** 891–913.
- KOHLER, M. and LANGER, S. (2021). On the rate of convergence of fully connected deep neural network regression estimates. *The Annals of Statistics* **49** 2231–2249.
- LECUN, Y., BENGIO, Y. and HINTON, G. (2015). Deep learning. *nature* **521** 436–444.
- LEE, A. J. (2019). *U-statistics: Theory and Practice*. Routledge.
- LEI, J., G’SSELL, M., RINALDO, A., TIBSHIRANI, R. J. and WASSERMAN, L. (2018). Distribution-free predictive inference for regression. *Journal of the American Statistical Association* **113** 1094–1111.
- LIPPI, G. and PLEBANI, M. (2014). Red blood cell distribution width (rdw) and human pathology. one size fits all. *Clinical Chemistry and Laboratory Medicine (CCLM)* **52** 1247–1249.
- LU, J., SHEN, Z., YANG, H. and ZHANG, S. (2021). Deep network approximation for smooth functions. *SIAM Journal on Mathematical Analysis* **53** 5465–5506.
- MCCAFFREY, D. F. and GALLANT, A. R. (1994). Convergence rates for single hidden layer feedforward networks. *Neural Networks* **7** 147–158.
- MENTCH, L. and HOOKER, G. (2016). Quantifying uncertainty in random forests via confidence intervals and hypothesis tests. *Journal of Machine Learning Research* **17** 1–41.
- NADARAYA, E. A. (1964). On estimating regression. *Theory of Probability & Its Applications* **9** 141–142.

- NAIR, V. and HINTON, G. E. (2010). Rectified linear units improve restricted boltzmann machines. In *Proceedings of the 27th international conference on machine learning (ICML-10)*.
- POLLARD, T. J., JOHNSON, A. E. W., RAFFA, J. D., CELI, L. A., MARK, R. G. and BADAWI, O. (2018). The eICU Collaborative Research Database, a freely available multi-center database for critical care research. *Scientific data* **5** 1–13.
- SCHMIDT-HIEBER, A. J. (2020). Nonparametric regression using deep neural networks with relu activation function. *Annals of statistics* **48** 1875–1897.
- SCHUPBACH, J., SHEPPARD, J. W. and FORRESTER, T. (2020). Quantifying uncertainty in neural network ensembles using u-statistics. In *2020 International Joint Conference on Neural Networks (IJCNN)*. IEEE.
- SHEN, G., JIAO, Y., LIN, Y. and HUANG, J. (2021). Robust nonparametric regression with deep neural networks. *arXiv preprint arXiv:2107.10343* .
- SHEN, Z., YANG, H. and ZHANG, S. (2019). Nonlinear approximation via compositions. *Neural Networks* **119** 74–84.
- TAKEZAWA, K. (2005). *Introduction to nonparametric regression*. John Wiley & Sons.
- VINCENT, J. L., BARON, J.-F., REINHART, K., GATTINONI, L., THIJS, L., WEBB, A., MEIER-HELLMANN, A., NOLLET, G., PERES-BOTA, D. and FOR THE ABC INVESTIGATORS (2002). Anemia and blood transfusion in critically ill patients. *JAMA* **288** 1499–1507.
- WAGER, S. and ATHEY, S. (2018). Estimation and inference of heterogeneous treatment effects using random forests. *Journal of the American Statistical Association* **113** 1228–1242.
- WANG, Q. and WEI, Y. (2022). Quantifying uncertainty of subsampling-based ensemble methods under a u-statistic framework. *Journal of Statistical Computation and Simulation* **92** 3706–3726.
- WANG, X., ZHOU, L. and LIN, H. (2024). Deep regression learning with optimal loss function. *Journal of the American Statistical Association* 1–13.
- YAN, S. and YAO, F. (2023). Nonparametric regression for repeated measurements with deep neural networks. *arXiv preprint arXiv:2302.13908* .
- YAROTSKY, D. (2017). Error bounds for approximations with deep ReLU networks. *Neural Networks* **94** 103–114.
- YAROTSKY, D. (2018). Optimal approximation of continuous functions by very deep relu networks. In *Conference On Learning Theory*.
- ZHANG, Y. and POLITIS, D. N. (2023). Bootstrap prediction intervals with asymptotic conditional validity and unconditional guarantees. *Information and Inference: A Journal of the IMA* **12** 157–209.
- ZHONG, Q., MUELLER, J. and WANG, J.-L. (2022). Deep learning for the partially linear cox model. *The Annals of Statistics* **50** 1348–1375.

A Proof of Theorems

A.1 Preliminaries

We present the following proposition and lemmas, which are used to prove Theorem 3.5. Let $\mathcal{N}_n(\tilde{\delta}, \mathcal{F}, \|\cdot\|_\infty)$ denote the covering number, i.e., the minimal number of $\|\cdot\|_\infty$ -balls with radius $\tilde{\delta}$ required to cover $\mathcal{F}(L, \mathbf{p}, s, F)$. For brevity, we write $\mathcal{N}_n = \mathcal{N}_n(\tilde{\delta}, \mathcal{F}, \|\cdot\|_\infty)$. Then, for any $\hat{f}_n \in \mathcal{F}(L, \mathbf{p}, s, F)$, we have the following result.

Proposition A.1. *Under the conditions of Theorem 3.5, there exist constants $c', C' > 0$ depending only on κ , the function ψ , F , and K , such that*

$$\begin{aligned} \frac{1}{2}\Delta_n(\hat{f}_n, f_0) - c' \left(\frac{\log \mathcal{N}_n}{n} + \left(\sqrt{\frac{\log \mathcal{N}_n}{n}} + 1 \right) \tilde{\delta} \right) &\leq R_n(\hat{f}_n, f_0) \leq 2\Delta_n(\hat{f}_n, f_0) \\ &+ 2 \inf_{f \in \mathcal{F}(L, \mathbf{p}, s, F)} \mathbb{E} \ell(\mathbf{X}; f, f_0) + C' \left(\frac{\log \mathcal{N}_n}{n} + \left(\sqrt{\frac{\log \mathcal{N}_n}{n}} + 1 \right) \tilde{\delta} \right). \end{aligned}$$

The proof is provided in the Supplementary Material. To obtain the bounds in Proposition A.1, we apply truncation techniques that account for heterogeneity across individuals, paving the way for establishing convergence results under generalized nonparametric regression models. The following two lemmas provide properties of the covering number and characterize the minimal distance between functions $f \in \mathcal{F}(L, \mathbf{p}, s, F)$ and f_0 .

Lemma A.2. *Let \mathcal{N}_n denote the covering number, i.e., the minimal number of $\|\cdot\|_\infty$ -balls with radius $\tilde{\delta}$ required to cover $\mathcal{F}(L, \mathbf{p}, s, \infty)$. Then*

$$\log(\mathcal{N}_n) \leq (s+1) \log \left(2\tilde{\delta}^{-1}(L+1) \left(\prod_{l=0}^{L+1} (1+p_l) \right)^2 \right).$$

Lemma A.3. *Under the conditions of Theorem 3.5, it holds that*

$$\inf_{f \in \mathcal{F}(L, \mathbf{p}, s, F)} \|f - f_0\|_\infty^2 \lesssim \phi_n.$$

Proofs of Lemmas A.2 and A.3. See Lemma 5 and the proof of Theorem 1 in Schmidt-Hieber (2020) for the proofs of Lemmas A.2 and A.3. \square

The following lemma establishes key properties of the function ψ in the context of generalized nonparametric regression models.

Lemma A.4. *Under Assumption 3.1, there exist constants $c', C', C_{\text{Lip}} > 0$ such that for any $x, m \in [-C, C]$, where $C > 0$,*

$$\frac{C'}{2}(x-m)^2 \geq \psi(x) - \psi(m) - \psi'(m)(x-m) \geq \frac{c'}{2}(x-m)^2, \quad \psi(x) - \psi(m) \leq C_{\text{Lip}}|x-m|.$$

A.2 Proof of Theorem 3.5

With Lemma A.2 and if we let $\tilde{\delta} = n^{-1}$, it holds that

$$\log(\mathcal{N}_n) \leq (s+1) \log \left(2n(L+1)(\max\{p_l\} + 1)^{2L+4} \right).$$

Combining this inequality with Assumption 3.3, we have $s \lesssim n\phi_n \log n$, $\max\{p_l\} \lesssim n$, and the upper bound of $\log(\mathcal{N}_n)$ can be written as

$$\log(\mathcal{N}_n) \lesssim n\phi_n L \log^2 n. \quad (\text{A.1})$$

By Proposition A.1, the lower bound for $R_n(\hat{f}_n, f_0)$ can be written as

$$\begin{aligned} \frac{1}{2}\Delta_n(\hat{f}_n, f_0) - R_n(\hat{f}_n, f_0) &\leq c' \left(\frac{\log \mathcal{N}_n}{n} + \left(\sqrt{\frac{\log \mathcal{N}_n}{n}} + 1 \right) n^{-1} \right) \\ &\lesssim \phi_n L \log^2 n. \end{aligned}$$

On the other hand, for the upper bound of $R_n(\hat{f}_n, f_0)$, Lemma A.3 yields

$$\inf_{f \in \mathcal{F}(L, \mathbf{p}, s, F)} \|f - f_0\|_\infty^2 \lesssim \phi_n.$$

From Lemma A.4, it follows that $\mathbb{E}\ell(\mathbf{X}; f, f_0) \lesssim \|f - f_0\|_\infty^2$. Hence, combining the upper bound of $\log(\mathcal{N}_n)$ in (A.1) and $\inf_{f \in \mathcal{F}(L, \mathbf{p}, s, F)} \|f - f_0\|_\infty^2$ above, we have

$$R_n(\hat{f}_n, f_0) - 2\Delta_n(\hat{f}_n, f_0) \lesssim \phi_n L \log^2 n.$$

A.3 Proof of Corollary 3.6

According to Theorem 3.5, we have that when $\Delta_n(\hat{f}^{b_j}, f_0) \leq C\phi_r L \log^2 r$,

$$R_n(\hat{f}^{b_j}, f_0) \lesssim \phi_r L \log^2 r.$$

Lemma A.4 further indicates that

$$R_n(\hat{f}^{b_j}, f_0) \geq \frac{c}{2} \mathbb{E}(\hat{f}^{b_j}(\mathbf{X}) - f_0(\mathbf{X}))^2.$$

Here, \mathbf{X} comes from the distribution $\mathbb{P}_{\mathbf{x}}$ independently, and the expectation is with respect to \mathbf{X} . Hence we have

$$\mathbb{E}(\hat{f}^{b_j}(\mathbf{X}) - f_0(\mathbf{X}))^2 \leq C\phi_r L \log^2 r$$

for some constant $C > 0$. By the inequality of $\mathbb{E}(\mathbb{E}(X|U) - U)^2 \leq \mathbb{E}(X - U)^2$ for any random variables X and U , we have the expectation

$$\mathbb{E}(\mathbb{E}\hat{f}^{b_j}(\mathbf{X})|\mathbf{X} - f_0(\mathbf{X}))^2 \leq C\phi_r L \log^2 r \rightarrow 0$$

for some constant $C > 0$. By the assumption $\lim_{n \rightarrow \infty} n\phi_r L \log^2(r)/(r^2 \inf_{\mathbf{x} \in \mathcal{X}} \xi_{1,r}(\mathbf{x})) = 0$ in Assumption 3.4, we have

$$\frac{n}{r^2 \inf_{\mathbf{x} \in \mathcal{X}} \xi_{1,r}(\mathbf{x})} \cdot \mathbb{E}|\mathbb{E}(\widehat{f}^B(\mathbf{X}) - f_0(\mathbf{X})|\mathbf{X})|^2 \rightarrow 0.$$

This completes the proof of Corollary 3.6.

A.4 Proof of Theorem 3.7

From the assumption of

$$\lim_{n \rightarrow \infty} n\phi_r L \log^2(r)/(r^2 \inf_{\mathbf{x} \in \mathcal{X}} \xi_{1,r}(\mathbf{x})) = 0,$$

there always exists a positive sequence δ_n with $\delta_n \rightarrow 0$ such that

$$\lim_{n \rightarrow \infty} n\phi_r L \log^2(r)/(\delta_n r^2 \inf_{\mathbf{x} \in \mathcal{X}} \xi_{1,r}(\mathbf{x})) = 0.$$

For such δ_n , we construct the set \mathcal{A}_{δ_n} as

$$\mathcal{A}_{\delta} = \left\{ \mathbf{X} \in \mathcal{X} : [\mathbb{E}\widehat{f}(\mathbf{X}) - f_0(\mathbf{X})|\mathbf{X}]^2 \leq \frac{C\phi_r L \log^2 r}{\delta_n} \right\},$$

By Chebyshev's inequality we have

$$\begin{aligned} \mathbb{P}_{\mathbf{x}}(\mathcal{A}_{\delta_n}) &= 1 - \mathbb{P}_{\mathbf{x}}\left([\mathbb{E}\widehat{f}(\mathbf{X}) - f_0(\mathbf{X})|\mathbf{X}]^2 \geq \frac{C\phi_r L \log^2 r}{\delta_n}\right) \\ &\geq 1 - \delta_n. \end{aligned}$$

Moreover, by the definition of \mathcal{A}_{δ_n} , we have for every fixed $\mathbf{x}_* \in \mathcal{A}_{\delta_n}$,

$$\sqrt{\frac{n}{r^2 \xi_{1,r}(\mathbf{x}_*)}} |\mathbb{E}(\widehat{f}^{b_j}(\mathbf{x}_*) - f_0(\mathbf{x}_*))| = O\left(\sqrt{\frac{n\phi_r L \log^2 r}{\delta_n r^2 \xi_{1,r}(\mathbf{x}_*)}}\right) \rightarrow 0,$$

where the last equality is by the condition $\lim_{n \rightarrow \infty} n\phi_r L \log^2(r)/(\delta_n r^2 \inf_{\mathbf{x} \in \mathcal{X}} \xi_{1,r}(\mathbf{x})) = 0$. By the basic inequality of $|\mathbb{E}\widehat{f}^B(\mathbf{x}_*) - f_0(\mathbf{x}_*)|^2 \leq \sum_{j=1}^B (\mathbb{E}\widehat{f}^{b_j}(\mathbf{x}_*) - f_0(\mathbf{x}_*))^2/B$, we have that

$$\sqrt{\frac{n}{r^2 \xi_{1,r}(\mathbf{x}_*)}} |\mathbb{E}(\widehat{f}^B(\mathbf{x}_*) - f_0(\mathbf{x}_*))| = O\left(\sqrt{\frac{n\phi_r L \log^2 r}{\delta_n r^2 \xi_{1,r}(\mathbf{x}_*)}}\right) \rightarrow 0 \quad (\text{A.2})$$

for any $\mathbf{x}_* \in \mathcal{A}_{\delta_n}$.

Assume the observed data of size n , $\mathcal{D}_n = \{(y_i, \mathbf{x}_i) : i = 1, \dots, n\}$, are independently and identically distributed copies of (y, \mathbf{X}) , with $y \in \mathbb{R}^1$ and $\mathbf{X} \in \mathbb{R}^{d \times 1}$. Let $\mathbf{z}_i = (y_i, \mathbf{x}_i)$ represent an independent observation of sample points, where y_i is the label and \mathbf{x}_i is the response. By the definition of $\xi_{1,r}(\mathbf{x})$, it is clear that

$$\xi_{1,r}(\mathbf{x}_*) = \text{Cov}(\widehat{f}(\mathbf{x}_*; \mathbf{z}_1, \mathbf{z}_2, \dots, \mathbf{z}_r), \widehat{f}(\mathbf{x}_*, \mathbf{z}_1, \mathbf{z}_2', \dots, \mathbf{z}_r')).$$

Here, $\widehat{f}(\mathbf{x}_*; \mathbf{z}_1, \mathbf{z}_2, \dots, \mathbf{z}_r)$ means that we obtain \widehat{f} from the subsample $\mathbf{z}_1, \mathbf{z}_2, \dots, \mathbf{z}_r$, and then apply

it to the point \mathbf{x}_* . The terms \mathbf{z}'_i and \mathbf{z}_i are independently generated from the same data generation process. In the following of the proofs, all the expectations and variance are taken over the fixed \mathbf{x}_* .

Next, we consider the asymptotic normality of the first order dominants of the Hoeffding decomposition. By the definition of $\hat{f}^B(\mathbf{x}_*)$, it is clear that \hat{f}^{b_j} and $\hat{f}^{b_{j'}}$ are not independent given \mathcal{I}^{b_j} and $\mathcal{I}^{b_{j'}}$ have overlap. To handle the dependency, we consider the Hoeffding decomposition. For the n sample data points $\mathbf{z}_i = (y_i, \mathbf{x}_i)$, define

$$\hat{f}^B(\mathbf{x}_*) = \sum_{i=1}^n \left(\mathbb{E}(\hat{f}^B(\mathbf{x}_*) | \mathbf{z}_i) - \mathbb{E}\hat{f}^b(\mathbf{x}_*) \right).$$

Here, the expectation \mathbb{E} is taken over the training sample. By the definition of $\hat{f}^B(\mathbf{x}_*)$, we have

$$\mathbb{E}(\hat{f}^B(\mathbf{x}_*) - (\mathbb{E}\hat{f}^b(\mathbf{x}_*)) | \mathbf{z}_i) = \mathbb{E}\left(\frac{1}{B} \sum_{j=1}^B \hat{f}^{b_j}(\mathbf{x}_*) | \mathbf{z}_i\right) - \mathbb{E}\hat{f}^b(\mathbf{x}_*).$$

Let W_{b_j} be the number of subsamples \mathcal{I}^{b_j} that contain index i , and define $g_{1,r}(x; \mathbf{x}_*) = \mathbb{E}\hat{f}^b(\mathbf{x}_*; x, \mathbf{z}_2, \dots, \mathbf{z}_r) - \mathbb{E}\hat{f}^b(\mathbf{x}_*)$. We have W_{b_j} is independent of \mathbf{z}_i and $\mathbb{E}W_{b_j} = B \binom{n-1}{r-1} / \binom{n}{r}$. Hence, the equation above involving the term \mathbf{z}_i can be further expressed as

$$\begin{aligned} & \mathbb{E}(\hat{f}^B(\mathbf{x}_*) - (\mathbb{E}\hat{f}^b(\mathbf{x}_*)) | \mathbf{z}_i) \\ &= \frac{1}{B} \sum_{j=1}^B \mathbb{E}_{W_{b_j}} \left(\mathbb{E}(\hat{f}^{b_j}(\mathbf{x}_*) - (\mathbb{E}\hat{f}^b(\mathbf{x}_*)) | \mathbf{z}_i, W_{b_j}) \right) \\ &= \frac{1}{B} \mathbb{E}_{W_{b_j}} W_{b_j} g_{1,r}(\mathbf{z}_i; \mathbf{x}_*) + \frac{1}{B} \mathbb{E}_{W_{b_j}} (B - W_{b_j}) \cdot \mathbb{E}(\hat{f}^{b_j}(\mathbf{x}_*) - \mathbb{E}\hat{f}^b(\mathbf{x}_*)) \\ &= \frac{r}{n} g_{1,r}(\mathbf{z}_i; \mathbf{x}_*). \end{aligned}$$

Therefore we conclude that

$$\hat{f}^B(\mathbf{x}_*) = \frac{r}{n} \sum_{i=1}^n g_{1,r}(\mathbf{z}_i; \mathbf{x}_*). \quad (\text{A.3})$$

Equation (A.3) provides a nice form, as $g_{1,r}(\mathbf{z}_i)$ is independent of each other. Moreover, by the assumption that \hat{f}^b is bounded, the Lindeberg condition is satisfied, and it is clear that

$$\frac{\sqrt{n}}{r \cdot \sqrt{\text{Var}(g_{1,r}(\mathbf{z}_i; \mathbf{x}_*))}} \cdot \hat{f}^B(\mathbf{x}_*) \xrightarrow{d} \mathcal{N}(0, 1).$$

By the definition of $\xi_{1,r}(\mathbf{x}_*)$, it is easy to see that $\text{Var}(g_{1,r}(\mathbf{z}_i; \mathbf{x}_*)) = \xi_{1,r}(\mathbf{x}_*)$, hence we have

$$\sqrt{\frac{n}{r^2 \xi_{1,r}(\mathbf{x}_*)}} \cdot \hat{f}^B(\mathbf{x}_*) \xrightarrow{d} \mathcal{N}(0, 1). \quad (\text{A.4})$$

In the next step, we would like to substitute $\hat{f}^B(\mathbf{x}_*)$ with $\hat{f}^B(\mathbf{x}_*) - \mathbb{E}\hat{f}^b(\mathbf{x}_*)$. Applying the

Hoeffding decomposition, it is clear that the simple $\hat{f}^b(\mathbf{x}_*; \mathbf{z}_1, \dots, \mathbf{z}_r)$ can be written as

$$\hat{f}^b(\mathbf{x}_*; \mathbf{z}_1, \dots, \mathbf{z}_r) - \mathbb{E}\hat{f}^b(\mathbf{x}_*) = \sum_{i=1}^r T_1(\mathbf{z}_i) + \sum_{i < j} T_2(\mathbf{z}_i, \mathbf{z}_j) \dots + T_r(\mathbf{z}_1, \dots, \mathbf{z}_r). \quad (\text{A.5})$$

The $2^r - 1$ random variables on the right hand side are all mean-zero and uncorrelated. Here, $T_1(\mathbf{z}_i) = \mathbb{E}(\hat{f}^b(\mathbf{x}_*; \mathbf{z}_1, \dots, \mathbf{z}_r) | \mathbf{z}_i) - \mathbb{E}\hat{f}^b(\mathbf{x}_*)$. Applying the decomposition to $\hat{f}^B(\mathbf{x}_*)$ and utilizing the same trick we obtain (A.3), we have

$$\begin{aligned} \mathbb{E}(\hat{f}^B(\mathbf{x}_*) - \mathbb{E}\hat{f}^b(\mathbf{x}_*) | \mathbf{z}_1, \dots, \mathbf{z}_n) &= \frac{1}{\binom{n}{r}} \left(\binom{n-1}{r-1} \sum_{i=1}^n T_1(\mathbf{z}_i) + \binom{n-2}{r-2} \sum_{i < j} T_2(\mathbf{z}_i, \mathbf{z}_j) \right. \\ &\quad \left. + \dots + \sum_{i_1 < \dots < i_r} T_r(\mathbf{z}_{i_1}, \dots, \mathbf{z}_{i_r}) \right). \end{aligned}$$

Hence, it is clear that $\hat{f}^B(\mathbf{x}_*)$ is exactly the first order in the Hoeffding decomposition. We have

$$\begin{aligned} &\mathbb{E}(\hat{f}^B(\mathbf{x}_*) - \mathbb{E}\hat{f}^b(\mathbf{x}_*) - \hat{f}^B(\mathbf{x}_*) | \mathbf{z}_1, \dots, \mathbf{z}_n) \\ &= \frac{1}{\binom{n}{r}} \left(\binom{n-2}{r-2} \sum_{i < j} T_2(\mathbf{z}_i, \mathbf{z}_j) + \dots + \sum_{i_1 < \dots < i_r} T_r(\mathbf{z}_{i_1}, \dots, \mathbf{z}_{i_r}) \right). \end{aligned}$$

Denote by $V_k = \text{Var}(T_k(\mathbf{z}_{i_1}, \dots, \mathbf{z}_{i_k}))$, we then calculate the value of $\mathbb{E}(\hat{f}^B(\mathbf{x}_*) - \mathbb{E}\hat{f}^b(\mathbf{x}_*) - \hat{f}^B(\mathbf{x}_*))^2$, which we will show later this term is negligible. To calculate this term, we apply the equality $\mathbb{E}X_n^2 = \mathbb{E}\text{Var}(X_n | Y_n) + \mathbb{E}(\mathbb{E}X_n | Y_n)^2$. Then the term $\mathbb{E}(\hat{f}^B(\mathbf{x}_*) - \mathbb{E}\hat{f}^b(\mathbf{x}_*) - \hat{f}^B(\mathbf{x}_*))^2$ can be written as

$$\begin{aligned} \mathbb{E}(\hat{f}^B(\mathbf{x}_*) - \mathbb{E}\hat{f}^b(\mathbf{x}_*) - \hat{f}^B(\mathbf{x}_*))^2 &= \underbrace{\mathbb{E}(\text{Var}(\hat{f}^B(\mathbf{x}_*) - \mathbb{E}\hat{f}^b(\mathbf{x}_*) - \hat{f}^B(\mathbf{x}_*) | \mathbf{z}_1, \dots, \mathbf{z}_n))}_{J_1} \\ &\quad + \underbrace{\mathbb{E}(\mathbb{E}(\hat{f}^B(\mathbf{x}_*) - \mathbb{E}\hat{f}^b(\mathbf{x}_*) - \hat{f}^B(\mathbf{x}_*) | \mathbf{z}_1, \dots, \mathbf{z}_n))^2}_{J_2}. \end{aligned}$$

Here, we let $X_n = \hat{f}^B(\mathbf{x}_*) - \mathbb{E}\hat{f}^b(\mathbf{x}_*) - \hat{f}^B(\mathbf{x}_*)$ and $Y_n = \mathbf{z}_1, \dots, \mathbf{z}_n$. From the expression of $\mathbb{E}(\hat{f}^B(\mathbf{x}_*) - \mathbb{E}\hat{f}^b(\mathbf{x}_*) - \hat{f}^B(\mathbf{x}_*) | \mathbf{z}_1, \dots, \mathbf{z}_n)$ above, we can easily see that

$$\begin{aligned} J_2 &= \frac{1}{\binom{n}{r}^2} \cdot \sum_{k=2}^r \binom{n-k}{r-k}^2 \cdot \binom{n}{k} V_k \\ &= \sum_{k=2}^r \frac{(n-k)!r!}{n!(r-k)!} \binom{r}{k} V_k \\ &\leq \frac{r(r-1)}{n(n-1)} \cdot \sum_{k=2}^r \binom{r}{k} V_k \\ &\leq \frac{r(r-1)}{n(n-1)} \text{Var}(\hat{f}^b(\mathbf{x}_*; \mathbf{z}_1, \dots, \mathbf{z}_r)). \end{aligned}$$

Here, the first equality is by the fact that all the terms are uncorrelated, the first inequality is by the

decreasing monotonicity of $\frac{(n-k)!r!}{n!(r-k)!}$ with respect to k , and the last inequality is by the decomposition of \hat{f}^b in (A.5). To calculate $\mathbb{E}(\hat{f}^B(\mathbf{x}_*) - \mathbb{E}\hat{f}^b(\mathbf{x}_*) - \hat{f}^B(\mathbf{x}_*))^2$, it remains for us to calculate J_1 . Let $W_{i_1 i_2 \dots i_k}$ ($k \leq r$) be the number of the B subsamples that contain index i_1, \dots, i_k simultaneously. Then we have

$$\hat{f}^B(\mathbf{x}_*) - \mathbb{E}\hat{f}^b(\mathbf{x}_*) - \hat{f}^B(\mathbf{x}_*) = \frac{1}{B} \left(\sum_{i_1 < i_2}^n W_{i_1 i_2} T_2(\mathbf{z}_{i_1}, \mathbf{z}_{i_2}) + \dots + \sum_{i_1 < \dots < i_r}^n W_{i_1 \dots i_r} T_r(\mathbf{z}_{i_1}, \dots, \mathbf{z}_{i_r}) \right).$$

By the independence on the different terms T_k , we conclude that

$$\begin{aligned} J_1 &= \frac{1}{B^2} \sum_{k=2}^r \text{Var}(W_{i_1 \dots i_k}) \binom{n}{k} V_k \\ &\leq \frac{1}{B} \sum_{k=2}^r \frac{\binom{n-k}{r-k}}{\binom{n}{r}} \binom{n}{k} V_k \\ &= \frac{1}{B} \sum_{k=2}^r \binom{r}{k} V_k \\ &\leq \frac{\text{Var}(\hat{f}^b(\mathbf{x}_*; \mathbf{z}_1, \dots, \mathbf{z}_r))}{B}. \end{aligned}$$

Here, the first inequality is by $\text{Var}(W_{i_1 \dots i_k}) \leq B \cdot \frac{\binom{n-k}{r-k}}{\binom{n}{r}}$ and the uncorrelation on different terms T_k , and the last inequality is by $\sum_{k=2}^r \binom{r}{k} V_k \leq \text{Var}(\hat{f}^b(\mathbf{x}_*; \mathbf{z}_1, \dots, \mathbf{z}_r))$. We hence conclude that

$$\begin{aligned} \mathbb{E}(\hat{f}^B(\mathbf{x}_*) - \mathbb{E}\hat{f}^b(\mathbf{x}_*) - \hat{f}^B(\mathbf{x}_*))^2 &= J_1 + J_2 \\ &\leq \left(\frac{r(r-1)}{n(n-1)} + \frac{1}{B} \right) \text{Var}(\hat{f}^b(\mathbf{x}_*; \mathbf{z}_1, \dots, \mathbf{z}_r)), \end{aligned}$$

leading to

$$\begin{aligned} \frac{n}{r^2 \xi_{1,r}(\mathbf{x}_*)} \cdot \mathbb{E}(\hat{f}^B(\mathbf{x}_*) - \mathbb{E}\hat{f}^b(\mathbf{x}_*) - \hat{f}^B(\mathbf{x}_*))^2 &\leq \left(\frac{1}{n \xi_{1,r}(\mathbf{x}_*)} + \frac{n}{B r^2 \xi_{1,r}(\mathbf{x}_*)} \right) \text{Var}(\hat{f}^b(\mathbf{x}_*; \mathbf{z}_1, \dots, \mathbf{z}_r)) \\ &\xrightarrow{p} 0. \end{aligned} \tag{A.6}$$

Here, we utilize the fact that $\hat{f}^b(\mathbf{x}_*)$ is bounded. The bound of $\hat{f}^b(\mathbf{x}_*)$ indicates that $\text{Var}(\hat{f}^b(\mathbf{x}_*; \mathbf{z}_1, \dots, \mathbf{z}_r))$ is bounded. Additionally, we rely on the assumption that $\liminf_{n \rightarrow +\infty} n \xi_{1,r}(\mathbf{x}_*) \rightarrow +\infty$ and $\liminf_{n \rightarrow +\infty} B r^2 \xi_{1,r}(\mathbf{x}_*)/n \rightarrow +\infty$. From (A.6), we have

$$\sqrt{\frac{n}{r^2 \xi_{1,r}(\mathbf{x}_*)}} \cdot (\hat{f}^B(\mathbf{x}_*) - \mathbb{E}\hat{f}^b(\mathbf{x}_*) - \hat{f}^B(\mathbf{x}_*)) \xrightarrow{p} 0.$$

Therefore it holds that

$$\sqrt{\frac{n}{r^2 \xi_{1,r}(\mathbf{x}_*)}} \cdot (\hat{f}^B(\mathbf{x}_*) - \mathbb{E}\hat{f}^b(\mathbf{x}_*) - \hat{f}^B(\mathbf{x}_*)) \xrightarrow{p} 0.$$

From (A.4), we also have that

$$\sqrt{\frac{n}{r^2 \xi_{1,r}(\mathbf{x}_*)}} \cdot \hat{f}^B(\mathbf{x}_*) \xrightarrow{p} \mathcal{N}(0, 1),$$

Combing the convergence above, we have

$$\sqrt{\frac{n}{r^2 \xi_{1,r}(\mathbf{x}_*)}} \cdot (\hat{f}^B(\mathbf{x}_*) - \mathbb{E} \hat{f}^b(\mathbf{x}_*)) \xrightarrow{d} \mathcal{N}(0, 1).$$

The only thing that needs to prove is

$$\sqrt{\frac{n}{r^2 \xi_{1,r}(\mathbf{x}_*)}} \cdot (f_0(\mathbf{x}_*) - \mathbb{E} \hat{f}^b(\mathbf{x}_*)) \rightarrow 0$$

for $\mathbf{x}_* \in \mathcal{A}_{\delta_n}$. This is proved by (A.2) and $\mathbb{E} \hat{f}^B(\mathbf{x}_*) = \mathbb{E} \hat{f}^b(\mathbf{x}_*)$. Wrapping all together, we complete the proof of Theorem 3.7.

A.5 Proof of Theorem 3.8

Recall the definition of

$$\hat{V}_i = \frac{\sum_{j=1}^B (J_{b_j i} - J_{\cdot i}) (\hat{f}^{b_j}(\mathbf{x}_*) - \hat{f}^B(\mathbf{x}_*))}{B}, \quad \hat{\sigma}_*^2 = \frac{n(n-1)}{(n-r)^2} \sum_{i=1}^n \hat{V}_i^2.$$

Without loss of generality, we calculate the term \hat{V}_1 , and the terms \hat{V}_i with $i \neq 1$ are exactly the same. Consider \hat{V}_1^2 as B/n tends to infinity. Then by the same combinatorics in the proof of Lemma 13 of Wager and Athey (2018), we can define

$$\begin{aligned} M_1 &= \left(\frac{r}{n} - \frac{r^2}{n^2} \right) T_1(\mathbf{z}_1) + \left(\frac{r(r-1)}{n(n-1)} - \frac{r^2}{n^2} \right) \sum_{i=2}^n T_1(\mathbf{z}_i) \\ &+ \frac{r}{n} \sum_{k=1}^{r-1} \left(\frac{\binom{r-1}{k}}{\binom{n-1}{k}} - \frac{\binom{r}{k+1}}{\binom{n}{k+1}} \right) \sum_{2 \leq i_1 < \dots < i_k \leq n} T_{k+1}(\mathbf{z}_1, \mathbf{z}_{i_1}, \dots, \mathbf{z}_{i_k}) \\ &+ \frac{r}{n} \sum_{k=2}^r \left(\frac{\binom{r-1}{k}}{\binom{n-1}{k}} - \frac{\binom{r}{k}}{\binom{n}{k}} \right) \sum_{2 \leq i_1 < \dots < i_k \leq n} T_k(\mathbf{z}_{i_1}, \dots, \mathbf{z}_{i_k}), \end{aligned}$$

and M_j the same way with 1 be replaced by j , and get that

$$\hat{\sigma}_*^2 \sim \frac{n(n-1)}{(n-r)^2} \sum_{i=1}^n M_i^2,$$

similar to the proof of Theorem 3.7 which relies on the Hoeffding decomposition on $\hat{f}^{b_j}(\mathbf{x}_*)$ and $\hat{f}^B(\mathbf{x}_*)$. Therefore, denoting by

$$\hat{\sigma}_1^2 = \frac{n(n-1)}{(n-r)^2} \sum_{i=1}^n M_i^2,$$

it remains for us to prove $\sqrt{\frac{r^2 \xi_{1,r}(\mathbf{x}_*)}{n \sigma_1^2}} \xrightarrow{p} 1$. All the terms T_k on the right hand side in M_i are uncorrelated. We define $A_1 = \left(\frac{r}{n} - \frac{r^2}{n^2}\right) T_1(\mathbf{z}_1) + \left(\frac{r(r-1)}{n(n-1)} - \frac{r^2}{n^2}\right) \sum_{i=2}^n T_1(\mathbf{z}_i)$ which is the first line of the equation above. We then have $\mathbb{E}(M_1 - A_1) \cdot A_1 = 0$. Similarly we define A_i with the replace of 1 by i . we give the calculation of three terms: $\mathbb{E}A_i \cdot T_1(\mathbf{z}_i)$, $\mathbb{E}A_i^2$ and $\mathbb{E}(M_i - A_i)^2$, and then give the proof based on these terms.

For the term $\mathbb{E}A_i \cdot T_1(\mathbf{z}_i)$, we have

$$\mathbb{E}A_i \cdot T_1(\mathbf{z}_i) = \mathbb{E}\left(\frac{r}{n} - \frac{r^2}{n^2}\right) T_1^2(\mathbf{z}_1) = \left(\frac{r}{n} - \frac{r^2}{n^2}\right) \xi_{1,r}(\mathbf{x}_*). \quad (\text{A.7})$$

For the term $\mathbb{E}A_i^2$, we have

$$\begin{aligned} \mathbb{E}A_i^2 &= \frac{r^2(n-r)^2}{n^4} \xi_{1,r}(\mathbf{x}_*) + \frac{r^2(n-1)}{n^2} \left(\frac{r-1}{n-1} - \frac{r}{n}\right)^2 \xi_{1,r}(\mathbf{x}_*) \\ &= \frac{r^2(n-r)^2}{n^3(n-1)} \xi_{1,r}(\mathbf{x}_*). \end{aligned} \quad (\text{A.8})$$

For the term $\mathbb{E}(\widehat{V}_i - A_i)^2$, we have

$$\begin{aligned} \mathbb{E}(M_i - A_i)^2 &= \frac{r^2}{n^2} \sum_{k=1}^{r-1} \binom{n-1}{k} \left(\frac{\binom{r-1}{k}}{\binom{n-1}{k}} - \frac{\binom{r}{k+1}}{\binom{n}{k+1}}\right)^2 V_{k+1} + \frac{r^2}{n^2} \sum_{k=2}^r \binom{n-1}{k} \left(\frac{\binom{r-1}{k}}{\binom{n-1}{k}} - \frac{\binom{r}{k}}{\binom{n}{k}}\right)^2 V_k \\ &\lesssim \frac{r^2(n-1)}{n^2} \left(\frac{r-1}{n-1} - \left(\frac{\binom{r}{2}}{\binom{n}{2}}\right)\right)^2 \binom{r}{2}^{-1} \text{Var}[\widehat{f}^b(\mathbf{x}_*)] \\ &\lesssim \frac{2r^2 \text{Var}[\widehat{f}^b(\mathbf{x}_*)]}{n^3}. \end{aligned} \quad (\text{A.9})$$

Here, the first inequality is by the fact that summation in the first line is maximized in the second-order terms and $\sum_{k=1}^r \binom{r}{k} V_k = \text{Var}(\widehat{f}^b(\mathbf{x}_*)) \leq C < +\infty$, and the second inequality is by simple calculation. We hence have

$$\begin{aligned} &\frac{n}{r^2 \xi_{1,r}(\mathbf{x}_*)} \cdot \mathbb{E} \frac{n(n-1)}{(n-r)^2} \sum_{i=1}^n \left(A_i - \frac{r(n-r)}{n^2} T_1(\mathbf{z}_i)\right)^2 \\ &= \frac{n^3(n-1)}{r^2(n-r)^2 \xi_{1,r}(\mathbf{x}_*)} \mathbb{E} \left(A_i - \frac{r(n-r)}{n^2} T_1(\mathbf{z}_i)\right)^2 \\ &= \frac{n^3(n-1)}{r^2(n-r)^2} \left(\frac{r^2(n-r)^2}{n^3(n-1)} - \frac{2r^2(n-r)^2}{n^4} + \frac{r^2(n-r)^2}{n^4}\right) \rightarrow 0. \end{aligned}$$

Here, the last equality comes from (A.7) and (A.8). For any sequence of random variable $X_n > 0$, $\mathbb{E}X_n \rightarrow 0$ implies $X_n \xrightarrow{p} 0$ by the Markov inequality. Therefore, we conclude that

$$\frac{n}{r^2 \xi_{1,r}(\mathbf{x}_*)} \cdot \frac{n(n-1)}{(n-r)^2} \sum_{i=1}^n \left(A_i - \frac{r(n-r)}{n^2} T_1(\mathbf{z}_i)\right)^2 \xrightarrow{p} 0. \quad (\text{A.10})$$

By the weak law of large number, we also have

$$\frac{n}{r^2 \xi_{1,r}(\mathbf{x}_*)} \cdot \frac{n(n-1)}{(n-r)^2} \sum_{i=1}^n \frac{r^2(n-r)^2}{n^4} T_1^2(\mathbf{z}_i) \xrightarrow{p} 1. \quad (\text{A.11})$$

Here $T_1^2(\mathbf{z}_i)$ are iid and the expectation $\mathbb{E}T_1^2(\mathbf{z}_i) = \xi_{1,r}(\mathbf{x}_*)$. We then investigate the convergence of the term

$$\frac{n}{r^2 \xi_{1,r}(\mathbf{x}_*)} \cdot \frac{n(n-1)}{(n-r)^2} \sum_{i=1}^n \frac{r}{n} A_i \cdot T_1(\mathbf{z}_i).$$

Recalling the definition of $A_i = \left(\frac{r}{n} - \frac{r^2}{n^2}\right)T_1(\mathbf{z}_i) + \left(\frac{r(r-1)}{n(n-1)} - \frac{r^2}{n^2}\right)\sum_{i' \neq i}^n T_1(\mathbf{z}_{i'})$, the equation above can be simplified and written as

$$\begin{aligned} \frac{n}{r^2 \xi_{1,r}(\mathbf{x}_*)} \cdot \frac{n(n-1)}{(n-r)^2} \sum_{i=1}^n \frac{r(n-r)}{n^2} A_i \cdot T_1(\mathbf{z}_i) &\sim \frac{n}{r(n-r)\xi_{1,r}(\mathbf{x}_*)} \sum_{i=1}^n A_i \cdot T_1(\mathbf{z}_i) \\ &= \frac{n}{r(n-r)\xi_{1,r}(\mathbf{x}_*)} \sum_{i=1}^n \left\{ \left(\frac{r}{n} - \frac{r^2}{n^2}\right)T_1^2(\mathbf{z}_i) + \left(\frac{r(r-1)}{n(n-1)} - \frac{r^2}{n^2}\right) \sum_{i' \neq i}^n T_1(\mathbf{z}_{i'})T_1(\mathbf{z}_i) \right\}. \end{aligned}$$

Again by utilizing the weak law of large number, we have

$$\frac{n}{r(n-r)\xi_{1,r}(\mathbf{x}_*)} \sum_{i=1}^n \left(\frac{r}{n} - \frac{r^2}{n^2}\right)T_1^2(\mathbf{z}_i) \xrightarrow{p} 1.$$

As for the term consisting of $T_1(\mathbf{z}_{i'})T_1(\mathbf{z}_i)$ above, we have

$$\begin{aligned} &\mathbb{E} \left\{ \frac{n}{r(n-r)\xi_{1,r}(\mathbf{x}_*)} \sum_{i=1}^n \left(\frac{r(r-1)}{n(n-1)} - \frac{r^2}{n^2}\right) \sum_{i' \neq i}^n T_1(\mathbf{z}_{i'})T_1(\mathbf{z}_i) \right\}^2 \\ &= \mathbb{E} \left\{ \frac{1}{n(n-1)\xi_{1,r}(\mathbf{x}_*)} \sum_{i=1}^n \sum_{i' \neq i}^n T_1(\mathbf{z}_{i'})T_1(\mathbf{z}_i) \right\}^2 \\ &= \frac{1}{n(n-1)} \rightarrow 0. \end{aligned}$$

Here, we use the fact $\mathbb{E}(\sum_{i' \neq i}^n T_1(\mathbf{z}_{i'})T_1(\mathbf{z}_i))^2 = n(n-1)\xi_{1,r}^2(\mathbf{x}_*)$ which follows from a straightforward calculation. This implies that the interaction term converges to 0 in probability. With these two terms, we have

$$\frac{n}{r^2 \xi_{1,r}(\mathbf{x}_*)} \cdot \frac{n(n-1)}{(n-r)^2} \sum_{i=1}^n \frac{r(n-r)}{n^2} A_i \cdot T_1(\mathbf{z}_i) \xrightarrow{p} 1. \quad (\text{A.12})$$

Combing (A.10) and (A.11) with (A.12), we have

$$\frac{n}{r^2 \xi_{1,r}(\mathbf{x}_*)} \cdot \frac{n(n-1)}{(n-r)^2} \sum_{i=1}^n A_i^2 \xrightarrow{p} 1.$$

Moreover, it follows from (A.9) that

$$\mathbb{E} \frac{n}{r^2 \xi_{1,r}(\mathbf{x}_*)} \cdot \frac{n(n-1)}{(n-r)^2} \sum_{i=1}^n (M_i - A_i)^2 \rightarrow 0,$$

which means

$$\frac{n}{r^2 \xi_{1,r}(\mathbf{x}_*)} \cdot \frac{n(n-1)}{(n-r)^2} \sum_{i=1}^n (M_i - A_i)^2 \xrightarrow{p} 0.$$

The triangle inequality implies that

$$\begin{aligned} \frac{n}{r^2 \xi_{1,r}(\mathbf{x}_*)} \cdot \frac{n(n-1)}{(n-r)^2} \sum_{i=1}^n M_i^2 &\leq \frac{n}{r^2 \xi_{1,r}(\mathbf{x}_*)} \cdot \frac{n(n-1)}{(n-r)^2} \left(\sum_{i=1}^n A_i^2 + \sum_{i=1}^n (M_i - A_i)^2 \right) \xrightarrow{p} 1, \\ \frac{n}{r^2 \xi_{1,r}(\mathbf{x}_*)} \cdot \frac{n(n-1)}{(n-r)^2} \sum_{i=1}^n M_i^2 &\geq \frac{n}{r^2 \xi_{1,r}(\mathbf{x}_*)} \cdot \frac{n(n-1)}{(n-r)^2} \left(\sum_{i=1}^n A_i^2 - \sum_{i=1}^n (M_i - A_i)^2 \right) \xrightarrow{p} 1. \end{aligned}$$

Hence, the squeeze theorem gives that

$$\frac{n}{r^2 \xi_{1,r}(\mathbf{x}_*)} \cdot \frac{n(n-1)}{(n-r)^2} \sum_{i=1}^n M_i^2 \xrightarrow{p} 1.$$

This completes the proof of Theorem 3.8.

B Proofs in Appendix A

We provide additional technical proofs for the conclusions in Appendix A. We first present the proof of Lemma A.4. Then we show several additional lemmas, which will be used to prove Proposition A.1.

Proof of Lemma A.4. By the definition we have

$$\psi(\eta) = \log \left(\int h(y) \exp(\eta y) dy \right),$$

and it is clear that

$$\mathbb{E}(Y|\eta) = \psi'(\eta), \quad \text{Var}(Y|\eta) = \psi''(\eta) \geq 0.$$

We conclude that $\psi(\cdot)$ is a convex function. By Assumption 3.1, the non-degeneracy and the existence of distinct values in the support of $p(y|\eta) = h(y) \exp(\eta y - \psi(\eta))$ ensure that $\text{Var}(Y|\eta) > 0$ for all $\eta \in [-C, C]$. This guarantees that the second derivative of the log-partition function, $\psi''(\eta) = \text{Var}(Y|\eta)$, is strictly positive. Furthermore, since $\mathbb{E}(Y|\eta)$ and $\mathbb{E}(Y^2|\eta)$ are defined as smooth integrals with respect to $p(y|\eta)$, they are continuous in η . As a result, $\psi''(\eta)$ is also continuous. By the compactness of $\eta \in [-C, C]$, there exists a constant $c > 0$ such that:

$$\psi''(\eta) \geq c > 0, \quad \text{for all } \eta \in [-C, C].$$

Using the second-order Taylor expansion and the definition of strong convexity, we establish:

$$\psi(x) - \psi(m) - \psi'(m)(x - m) = \frac{\psi''(\xi)}{2}(x - m)^2,$$

for some ξ between x and m . Since $C' \geq \psi''(\xi) \geq c' > 0$, we conclude:

$$\frac{C'}{2}(x - m)^2 \geq \psi(x) - \psi(m) - \psi'(m)(x - m) \geq \frac{c'}{2}(x - m)^2.$$

As for the Lipchitz property, by the equation $\psi'(\eta) = \mathbb{E}(Y|\eta)$, the bound of $\psi'(\eta)$ directly comes from the existence of the expectation of Y given η . \square

We propose several lemmas to address the general nonparametric regression cases, serving as the basis for the proof of Proposition A.1. Recall the definition of $R_n(\hat{f}_n, f_0)$ in (2.6):

$$R_n(\hat{f}_n, f_0) = \mathbb{E}[\ell(\mathbf{X}; \hat{f}_n, f_0)],$$

and consider the construction of

$$\hat{R}_n(\hat{f}_n, f_0) = \mathbb{E}\left[\frac{1}{n} \sum_{i=1}^n \ell(\mathbf{x}_i; \hat{f}_n, f_0)\right].$$

In the following lemmas, we demonstrate that the differences between $R_n(\hat{f}_n, f_0)$ and $\hat{R}_n(\hat{f}_n, f_0)$ are small. Some of the proof techniques are inspired by Schmidt-Hieber (2020), but our analysis extends to a more general regression framework, and our proofs differ accordingly. In fact, the settings considered by Schmidt-Hieber (2020) are special cases within our broader context. Additionally, we provide upper and lower bounds for $\hat{R}_n(\hat{f}_n, f_0)$. These results will be used for proving Proposition A.1.

Lemma B.1. *Under Assumptions 3.1, it holds that*

$$\begin{aligned} |\hat{R}_n(\hat{f}_n, f_0) - R_n(\hat{f}_n, f_0)| &\leq \frac{2R}{n} R_n^{1/2}(\hat{f}_n, f_0) \sqrt{9n \log \mathcal{N}_n + 4n \cdot \frac{1 + 3 \log \mathcal{N}_n}{\log \mathcal{N}_n}} \\ &\quad + \frac{2R(3 \log \mathcal{N}_n + 2)}{n} + 5\tilde{\delta} C_{\text{Lip}}. \end{aligned}$$

Here, \mathcal{N}_n is the minimum number of $\tilde{\delta}$ -covering of $\mathcal{F}(L, \mathbf{p}, s, \infty)$, and $R = 3FC_{\text{Lip}}$ is a constant assumed larger than 1 without loss of generality.

Lemma B.1 establishes the differences between $R_n(\hat{f}_n, f_0)$ and $\hat{R}_n(\hat{f}_n, f_0)$. We now propose the following lemma, which addresses the challenges arising from the dependency of ε_i on the covariates \mathbf{x}_i . This approach is different from previous work, such as Schmidt-Hieber (2020) and Fan and Gu (2024), which assumed independence between ε_i and \mathbf{x}_i .

Lemma B.2. *Suppose that Assumptions 3.1 and 3.2 hold. Define $\varepsilon_i = y_i - \psi'(f_0(\mathbf{x}_i))$. For any estimator $\tilde{f} \in \mathcal{F}$, there exists constant $C > 0$ such that*

$$\left| \mathbb{E} \frac{1}{n} \sum_{i=1}^n \varepsilon_i \tilde{f}(\mathbf{x}_i) \right| \leq \sqrt{\frac{2C \hat{R}_n(\tilde{f}, f_0) \log \mathcal{N}_n}{n}} + \sqrt{2C} \left(\frac{\log \mathcal{N}_n}{n} + \sqrt{\frac{\log \mathcal{N}_n}{n}} \tilde{\delta} \right) + 2\tilde{\delta} C.$$

The main difficulty in Lemma B.2 is the dependence of ε_i and \mathbf{x}_i under the GNRM framework. Unlike traditional concentration inequalities, here we apply covering number analysis and truncation techniques to address the heteroskedasticity in GNRMs. Details can be referred to Section B.2. With Lemma B.2, we establish the following two lemmas, which provides the upper and lower bound of $\widehat{R}_n(\widehat{f}_n, f_0)$.

Lemma B.3. *Suppose that Assumptions 3.1 and 3.2 hold. For any fixed $f \in \mathcal{F}$, it holds that*

$$\widehat{R}_n(\widehat{f}_n, f_0) \leq \inf_{f \in \mathcal{F}} \mathbb{E} \ell(\mathbf{X}; f, f_0) + \sqrt{\frac{2C \widehat{R}_n(\widehat{f}, f_0) \log \mathcal{N}_n}{n}} + \sqrt{2C} \left(\frac{\log \mathcal{N}_n}{n} + \sqrt{\frac{\log \mathcal{N}_n}{n}} \widetilde{\delta} \right) + 2\widetilde{\delta}C + \Delta_n(\widehat{f}_n, f_0).$$

Here, \mathbf{X} is an independent copy of \mathbf{x}_i and $C > 0$ is a constant.

Lemma B.4. *Suppose that Assumptions 3.1 and 3.2 hold. It holds that*

$$\widehat{R}_n(\widehat{f}_n, f_0) \geq \frac{1}{1+\rho} \cdot \left(\Delta_n(\widehat{f}_n, f_0) - 2\sqrt{2C} \left(\frac{\log \mathcal{N}_n}{n} + \sqrt{\frac{\log \mathcal{N}_n}{n}} \widetilde{\delta} \right) - 4\widetilde{\delta}C - \frac{C \log \mathcal{N}_n}{2n} \right)$$

for any $\rho > 0$. Here, $C > 0$ is a constant.

B.1 Proof of Lemma B.1

Given a minimum $\widetilde{\delta}$ -covering of \mathcal{F} , let the center of the balls by f_j . Recall $\mathcal{D}_n = \{(\mathbf{x}_i, y_i), i \in [n]\}$. By construction there exists a j^* such that $\|\widehat{f} - f_{j^*}\|_\infty \leq \widetilde{\delta}$. Moreover, by the assumptions we have $\|f_j\|_\infty \leq F$. Suppose that \mathbf{X}'_i ($i \in [n]$) are i.i.d random variables with the same distribution of \mathbf{X} and independent of the sample $(\mathbf{x}_i)_{i \in [n]}$ (\mathcal{D}_n) and recall

$$\ell(\mathbf{x}; \widehat{f}_n, f_0) = -\psi'(f_0(\mathbf{x}))\widehat{f}_n(\mathbf{x}) + \psi(\widehat{f}_n(\mathbf{x})) + \psi'(f_0(\mathbf{x}))f_0(\mathbf{x}) - \psi(f_0(\mathbf{x})).$$

It is clear to see that $\ell(\mathbf{x}; \widehat{f}_n, f_0) \geq 0$ by Lemma A.4, and

$$\begin{aligned} & |R_n(\widehat{f}_n, f_0) - \widehat{R}_n(\widehat{f}_n, f_0)| \\ &= \left| \mathbb{E} \left\{ \frac{1}{n} \sum_{i=1}^n \left[\ell(\mathbf{X}'_i; \widehat{f}_n, f_0) - \ell(\mathbf{x}_i; \widehat{f}_n, f_0) \right] \right\} \right|. \end{aligned}$$

Rewriting the equation above by $\widehat{f}_n = \widehat{f}_n - f_{j^*} + f_{j^*}$, we have the inequality for any $\|\widehat{f}_n - f_{j^*}\|_\infty \leq \widetilde{\delta}$,

$$|\ell(\mathbf{x}; \widehat{f}_n, f_0) - \ell(\mathbf{x}; f_{j^*}, f_0)| \leq 2\widetilde{\delta}C_{\text{Lip}},$$

and hence

$$|R_n(\widehat{f}_n, f_0) - \widehat{R}_n(\widehat{f}_n, f_0)| \leq \mathbb{E} \left\{ \left| \frac{1}{n} \sum_{i=1}^n g_{j^*}(\mathbf{X}'_i, \mathbf{x}_i) \right| \right\} + 4\widetilde{\delta}C_{\text{Lip}}, \quad (\text{B.1})$$

where

$$g_{j^*}(\mathbf{X}'_i, \mathbf{x}_i) = \ell(\mathbf{X}'_i; f_{j^*}, f_0) - \ell(\mathbf{x}_i; f_{j^*}, f_0). \quad (\text{B.2})$$

We define g_j the same way with f_{j^*} replaced with f_j . By letting $U = \mathbb{E}^{1/2}\{\ell(\mathbf{X}; \widehat{f}_n, f_0) | \mathcal{D}_n\}$, it is clear that

$$\begin{aligned} \left| \sum_{i=1}^n g_{j^*}(\mathbf{X}'_i, \mathbf{x}_i) \right| &= \frac{\left| \sum_{i=1}^n g_{j^*}(\mathbf{X}'_i, \mathbf{x}_i) \right|}{\max\{\sqrt{\log \mathcal{N}_n/n}, \mathbb{E}^{1/2}[\ell(\mathbf{X}; f_{j^*}, f_0) | \mathcal{D}_n]\}} \cdot \max\{\sqrt{\log \mathcal{N}_n/n}, \mathbb{E}^{1/2}[\ell(\mathbf{X}; f_{j^*}, f_0) | \mathcal{D}_n]\} \\ &\leq \max_j \frac{\left| \sum_{i=1}^n g_j(\mathbf{X}'_i, \mathbf{x}_i) \right|}{\max\{\sqrt{\log \mathcal{N}_n/n}, \mathbb{E}^{1/2}[\ell(\mathbf{X}; f_j, f_0)]\}} \cdot \left(\sqrt{\log \mathcal{N}_n/n} + U + \widetilde{\delta} C_{\text{Lip}} \right), \end{aligned}$$

where the second inequality comes from the fact $\|f_{j^*} - \widehat{f}_n\|_\infty \leq \widetilde{\delta}$, and hence $\mathbb{E}^{1/2}[\ell(\mathbf{X}; f_{j^*}, f_0) | \mathcal{D}_n] \leq U + 2\widetilde{\delta} C_{\text{Lip}}$. Define the random variable

$$T = \max_j \frac{\left| \sum_{i=1}^n g_j(\mathbf{X}'_i, \mathbf{x}_i) \right|}{\max\{\sqrt{\log \mathcal{N}_n/n}, \mathbb{E}^{1/2}[\ell(\mathbf{X}; f_j, f_0)]\}},$$

and it follows from (B.1) and the inequality above that

$$|R_n(\widehat{f}_n, f_0) - \widehat{R}_n(\widehat{f}_n, f_0)| \leq \mathbb{E} \frac{T}{n} \cdot \left(\sqrt{\log \mathcal{N}_n/n} + U + 2\widetilde{\delta} C_{\text{Lip}} \right) + 4\widetilde{\delta} C_{\text{Lip}}. \quad (\text{B.3})$$

Hence, it remains for us to consider the bound of (B.3). By the definition of $g_j(\mathbf{X}'_i, \mathbf{x}_i)$, it is clear that $\mathbb{E} g_j(\mathbf{X}'_i, \mathbf{x}_i) = 0$,

$$0 \leq \ell(\mathbf{x}; f_j, f_0) \leq R,$$

and hence $|g_j(\mathbf{X}'_i, \mathbf{x}_i)| \leq 2R$. Moreover, we have that

$$\begin{aligned} \text{Var}(g_j(\mathbf{X}'_i, \mathbf{x}_i)) &= 2 \text{Var}(\ell(\mathbf{X}; f_j, f_0)) \\ &\leq 2\mathbb{E} \ell^2(\mathbf{X}; f_j, f_0) \leq 2R \mathbb{E} \ell(\mathbf{X}; f_j, f_0). \end{aligned}$$

As $g_j(\mathbf{X}'_i, \mathbf{x}_i)$ is independent with different i , then for any i.i.d bounded and centered random variables ξ_i with $|\xi_i| \leq M$, the Bernstein inequality shows that

$$\mathbb{P}(|\sum_{i=1}^n \xi_i| \geq t_0) \leq 2 \exp \left(- \frac{t_0^2}{2Mt_0/3 + 2 \sum_{i=1}^n \text{Var}(\xi_i)} \right).$$

Combining the Bernstein inequality with the expression of T , we can apply the union bound and get that

$$\mathbb{P}(T/R \geq t) \leq 2\mathcal{N}_n \cdot \exp \left(- \frac{t^2}{\frac{4}{3}t \max^{-1}\{\sqrt{\log \mathcal{N}_n/n}, \mathbb{E}^{1/2}[\ell(\mathbf{X}; f_j, f_0)]\} + 4n/R} \right).$$

Here, we take $\xi_i = g_j(\mathbf{X}'_i, \mathbf{x}_i)/R$, and let $t_0 = t \max\{\sqrt{\log \mathcal{N}_n/n}, \mathbb{E}^{1/2}[\ell(\mathbf{X}; f_j, f_0)]\}$. According to (B.4), we can bound the value of $\mathbb{E}T$ and $\mathbb{E}T^2$, which will further be applied in (B.3). With the assumption above, we have $R \geq 1$, and the equation above can be simplified as

$$\mathbb{P}(T/R \geq t) \leq 2\mathcal{N}_n \cdot \exp \left(- \frac{t^2}{\frac{4}{3}t \max^{-1}\{\sqrt{\log \mathcal{N}_n/n}, \mathbb{E}^{1/2}[\ell(\mathbf{X}; f_j, f_0)]\} + 4n} \right). \quad (\text{B.4})$$

For the bound of $\mathbb{E}T/R$, it holds that

$$\begin{aligned}
\mathbb{E}T/R &= \mathbb{E}T/R \cdot \mathbf{1}\{T/R \leq 6\sqrt{n \log \mathcal{N}_n}\} + \mathbb{E}T/R \cdot \mathbf{1}\{T/R \geq 6\sqrt{n \log \mathcal{N}_n}\} \\
&= 6\sqrt{n \log \mathcal{N}_n} + \int_{6\sqrt{n \log \mathcal{N}_n}}^{+\infty} \mathbb{P}(T \geq t) dt \\
&\leq 6\sqrt{n \log \mathcal{N}_n} + \int_{6\sqrt{n \log \mathcal{N}_n}}^{+\infty} 2\mathcal{N}_n \exp\left(-\frac{t\sqrt{\log \mathcal{N}_n}}{2\sqrt{n}}\right) dt \\
&= 6\sqrt{n \log \mathcal{N}_n} + 4\sqrt{\frac{n}{\log \mathcal{N}_n}}.
\end{aligned} \tag{B.5}$$

Here, the inequality comes from (B.4) that when $t \geq 6\sqrt{n \log \mathcal{N}_n}$, $\mathbb{P}(T/R > t) \leq 2\mathcal{N}_n \exp\left(-\frac{t\sqrt{\log \mathcal{N}_n}}{2\sqrt{n}}\right)$, and the last inequality is by some algebra.

For the bound of $\mathbb{E}T^2/R^2$, it holds that

$$\begin{aligned}
\mathbb{E}T^2/R^2 &= \mathbb{E}T^2/R^2 \cdot \mathbf{1}\{T^2/R^2 \leq 6^2 n \log \mathcal{N}_n\} + \mathbb{E}T^2/R^2 \cdot \mathbf{1}\{T^2/R^2 \geq 6^2 n \log \mathcal{N}_n\} \\
&= 6^2 n \log \mathcal{N}_n + \int_{6^2 n \log \mathcal{N}_n}^{+\infty} \mathbb{P}(T \geq \sqrt{t}) dt \\
&\leq 6^2 n \log \mathcal{N}_n + \int_{6^2 n \log \mathcal{N}_n}^{+\infty} 2\mathcal{N}_n \exp\left(-\frac{\sqrt{t}\sqrt{\log \mathcal{N}_n}}{2\sqrt{n}}\right) dt \\
&= 36 n \log \mathcal{N}_n + 16 \cdot \frac{1 + 3 \log \mathcal{N}_n}{\log \mathcal{N}_n}.
\end{aligned} \tag{B.6}$$

Here, the inequality comes from (B.4) that when $t \geq 6\sqrt{n \log \mathcal{N}_n}$, $\mathbb{P}(T/R > t) \leq 2\mathcal{N}_n \exp\left(-\frac{t\sqrt{\log \mathcal{N}_n}}{(4/3+4/(2R+2))\sqrt{n}}\right)$, and the last equality is by $\int_{b^2}^{+\infty} e^{-\sqrt{t}a} dt = 2(ab+1)e^{-ab}/a^2$.

Combining (B.5), (B.6) with (B.3), and noting that $\mathbb{E}U^2 = R_n(\hat{f}_n, f_0)$ where U is defined below (B.2), we have

$$\begin{aligned}
|R_n(\hat{f}_n, f_0) - \hat{R}_n(\hat{f}_n, f_0)| &\leq \mathbb{E}T \cdot \left(\sqrt{\log \mathcal{N}_n/n} + U + \tilde{\delta}C_{\text{Lip}}\right) + 4\tilde{\delta}C_{\text{Lip}} \\
&\leq \frac{1}{n}\mathbb{E}^{1/2}T^2 \cdot \mathbb{E}^{1/2}U^2 + \mathbb{E}\frac{T}{n} \cdot \left(\sqrt{\log \mathcal{N}_n/n} + \tilde{\delta}C_{\text{Lip}}\right) + 4\tilde{\delta}C_{\text{Lip}} \\
&\leq \frac{2R}{n}R_n^{1/2}(\hat{f}_n, f_0)\sqrt{9n \log \mathcal{N}_n + 4n \cdot \frac{1 + 3 \log \mathcal{N}_n}{\log \mathcal{N}_n}} \\
&\quad + \frac{2R}{n}\left(3\sqrt{n \log \mathcal{N}_n} + 2\sqrt{\frac{n}{\log \mathcal{N}_n}}\right) \cdot (\sqrt{\log \mathcal{N}_n/n} + 2\tilde{\delta}C_{\text{Lip}}) + 4\tilde{\delta}C_{\text{Lip}} \\
&\leq \frac{2R}{n}R_n^{1/2}(\hat{f}_n, f_0)\sqrt{9n \log \mathcal{N}_n + 4n \cdot \frac{1 + 3 \log \mathcal{N}_n}{\log \mathcal{N}_n}} + \frac{2R(3 \log \mathcal{N}_n + 2)}{n} + 5\tilde{\delta}C_{\text{Lip}}.
\end{aligned}$$

Here, the first inequality is by the Cauchy-Schwarz inequality, the second inequality is by (B.5) and (B.6) and the last inequality holds when n is large enough.

B.2 Proof of Lemma B.2

For any estimator \tilde{f} taking values in \mathcal{F} , let j' be such that $\|\tilde{f} - f_{j'}\|_\infty \leq \tilde{\delta}$. We have

$$\begin{aligned} \left| \mathbb{E} \frac{1}{n} \sum_{i=1}^n \varepsilon_i \tilde{f}(\mathbf{x}_i) \right| &= \left| \mathbb{E} \frac{1}{n} \sum_{i=1}^n \varepsilon_i (\tilde{f}(\mathbf{x}_i) - f_{j'}(\mathbf{x}_i) + f_{j'}(\mathbf{x}_i)) \right| \\ &\leq \frac{\tilde{\delta}}{n} \mathbb{E} \sum_{i=1}^n |\varepsilon_i| + \frac{1}{n} \left| \mathbb{E} \sum_{i=1}^n \varepsilon_i f_{j'}(\mathbf{x}_i) \right| \\ &\leq 2\tilde{\delta}C + \frac{1}{n} \left| \mathbb{E} \sum_{i=1}^n \varepsilon_i f_{j'}(\mathbf{x}_i) \right|. \end{aligned} \quad (\text{B.7})$$

Here, C is some large constant. the first inequality is by the triangle inequality, and the second inequality is by $\mathbb{E}|\varepsilon_i| = \mathbb{E}\{\mathbb{E}\{|y_i - \psi'(f_0(\mathbf{x}_i))|\}|\mathbf{x}_i\}\} \leq L + \mathbb{E}|Y| \leq C$ for some large constant C . It is remained for us to bound the last term above. To obtain the bound, we first introduce $r_j = \sqrt{\frac{\log \mathcal{N}_n}{n}} \vee \sqrt{\sum_{i=1}^n (f_j(\mathbf{x}_i) - f_0(\mathbf{x}_i))^2/n}$. Then the term can be written as

$$\begin{aligned} \frac{1}{n} \left| \mathbb{E} \sum_{i=1}^n \varepsilon_i f_{j'}(\mathbf{x}_i) \right| &= \frac{1}{n} \left| \mathbb{E} \sum_{i=1}^n \varepsilon_i (f_{j'}(\mathbf{x}_i) - f_0(\mathbf{x}_i)) \right| \\ &\leq \frac{1}{n} \cdot \mathbb{E} \left[\left(\sqrt{\frac{\log \mathcal{N}_n}{n}} + \sqrt{\sum_{i=1}^n (f_{j'}(\mathbf{x}_i) - f_0(\mathbf{x}_i))^2/n} \right) \cdot \frac{\left| \sum_{i=1}^n \varepsilon_i (f_{j'}(\mathbf{x}_i) - f_0(\mathbf{x}_i)) \right|}{r_{j'}} \right] \\ &\leq \frac{1}{n} \cdot \mathbb{E} \left[\left(\sqrt{\frac{\log \mathcal{N}_n}{n}} + \sqrt{\sum_{i=1}^n (\tilde{f}(\mathbf{x}_i) - f_0(\mathbf{x}_i))^2/n} + \tilde{\delta} \right) \cdot \frac{\left| \sum_{i=1}^n \varepsilon_i (f_{j'}(\mathbf{x}_i) - f_0(\mathbf{x}_i)) \right|}{r_{j'}} \right] \\ &\leq \frac{1}{n} \left(\sqrt{\frac{\log \mathcal{N}_n}{n}} + \mathbb{E}^{1/2} \left(\frac{\sum_{i=1}^n \ell(\mathbf{x}_i; \tilde{f}, f_0)}{cn} \right) + \tilde{\delta} \right) \cdot \mathbb{E}^{1/2} \frac{\left| \sum_{i=1}^n \varepsilon_i (f_{j'}(\mathbf{x}_i) - f_0(\mathbf{x}_i)) \right|^2}{r_{j'}^2} \\ &= \frac{1}{n} \left(\sqrt{\frac{\log \mathcal{N}_n}{n}} + \hat{R}_n^{1/2}(\tilde{f}, f_0)/\sqrt{c} + \tilde{\delta} \right) \cdot \mathbb{E}^{1/2} \frac{\left| \sum_{i=1}^n \varepsilon_i (f_{j'}(\mathbf{x}_i) - f_0(\mathbf{x}_i)) \right|^2}{r_{j'}^2}. \end{aligned} \quad (\text{B.8})$$

Here, the first equality is by $\mathbb{E}\varepsilon_i f_0(\mathbf{x}_i) = \mathbb{E}(\mathbb{E}\varepsilon_i f_0(\mathbf{x}_i)|\mathbf{x}_i) = 0$, the first inequality is by $r_j \leq \frac{\log \mathcal{N}_n}{n} + \sqrt{\sum_{i=1}^n (f_j(\mathbf{x}_i) - f_0(\mathbf{x}_i))^2/n}$, the second inequality is by triangle inequality $\|\mathbf{a} + \mathbf{b}\| \leq \|\mathbf{a}\| + \|\mathbf{b}\|$ and $\|f_{j'} - \tilde{f}\|_\infty \leq \tilde{\delta}$, and the last inequality is by Lemma A.4 that $\ell(\mathbf{x}; \tilde{f}, f_0) \geq c(\tilde{f}(\mathbf{x}) - f_0(\mathbf{x}))^2$ for some constant $c > 0$.

It remains for us to bound $\mathbb{E}^{1/2} \frac{\left| \sum_{i=1}^n \varepsilon_i (f_{j'}(\mathbf{x}_i) - f_0(\mathbf{x}_i)) \right|^2}{r_{j'}^2}$. The heteroskedasticity in GNRMs also makes the bound of this term complicated, mainly due to the dependence among ε_i and \mathbf{x}_i . For simplicity in notation, define

$$\xi_j = \frac{\left| \sum_{i=1}^n \varepsilon_i (f_j(\mathbf{x}_i) - f_0(\mathbf{x}_i)) \right|}{r_j}. \quad (\text{B.9})$$

We investigate the noise behavior ξ_j^2 under different regimes to bound the term with heteroskedas-

ticity. Specifically, we consider $\max_{j \in [\mathcal{N}_n]} \xi_j^2 \leq Cn \log \mathcal{N}_n$ and $\max_{j \in [\mathcal{N}_n]} \xi_j^2 \geq Cn \log \mathcal{N}_n$ conditional on \mathbf{x}_i . When $\max_{j \in [\mathcal{N}_n]} \xi_j^2 \leq Cn \log \mathcal{N}_n$ conditional on \mathbf{x}_i , the results will obviously hold. We mainly focus the regime when $\max_{j \in [\mathcal{N}_n]} \xi_j^2 \geq Cn \log \mathcal{N}_n$ conditional on \mathbf{x}_i . Conditional on $\mathbf{x}_1, \dots, \mathbf{x}_n$ [or $(\mathbf{x}_i)_i$ compactly], we have that ε_i 's ($i \in [n]$) are centered and independent sub-exponential random variables. Hence, we have

$$\begin{aligned} \text{Var}(\xi_j | (\mathbf{x}_i)_i) &= \frac{\sum_{i=1}^n \text{Var}(\varepsilon_i(f_j(\mathbf{x}_i) - f_0(\mathbf{x}_i)) | (\mathbf{x}_i)_i)}{r_j^2} \\ &\leq \sum_{i=1}^n \mathbb{E}(\varepsilon_i^2 | (\mathbf{x}_i)_i) \cdot \mathbb{E}((f_j(\mathbf{x}_i) - f_0(\mathbf{x}_i))^2 | (\mathbf{x}_i)_i) / r_j^2 \\ &\leq 2n\kappa^2, \end{aligned}$$

where the first inequality is by $\text{Var}(U|X) \leq \mathbb{E}(U^2|X)$ for all random variables X and U , and the second inequality is by the definition of $r_j = \sqrt{\frac{\log \mathcal{N}_n}{n}} \vee \sqrt{\sum_{i=1}^n (f_j(\mathbf{x}_i) - f_0(\mathbf{x}_i))^2 / n}$, and $\mathbb{E}(\varepsilon_i^2 | (\mathbf{x}_i)_i) \leq 2\kappa^2$. Also, letting $a_{ij} = [f_j(\mathbf{x}_i) - f_0(\mathbf{x}_i)] / r_j$, we have

$$|a_{ij}| \leq 2F/r_j, \quad \sum_{i=n}^n a_{ij}^2 \leq n.$$

Therefore by the Bernstein inequality, it holds that

$$\mathbb{P}(|\xi_j| \geq t | (\mathbf{x}_i)_i) \leq 2 \exp \left\{ -c' \min \left\{ \frac{t^2}{n\kappa^2}, \frac{tr_j}{2F\kappa} \right\} \right\}$$

for some absolute constant $c' > 0$.

Let $\xi_{\max} = \max_{j \in [\mathcal{N}_n]} \xi_j$. By applying the union bound, it holds that

$$\begin{aligned} \mathbb{E}(|\xi_{\max}|^2 | (\mathbf{x}_i)_i) &= \int_0^{+\infty} \mathbb{P}(|\xi_{\max}|^2 \geq t | (\mathbf{x}_i)_i) dt \\ &\leq T + \int_T^{+\infty} \mathbb{P}(|\xi_{\max}| \geq \sqrt{t} | (\mathbf{x}_i)_i) dt \\ &\leq T + \mathcal{N}_n \cdot \int_T^{+\infty} 2 \exp \left\{ -c' \min \left\{ \frac{t}{n\kappa^2}, \frac{\sqrt{t}r_j}{2F\kappa} \right\} \right\} dt \\ &\leq T + \mathcal{N}_n \cdot \int_T^{+\infty} 2 \exp \left\{ -c' \min \left\{ \frac{t}{n\kappa^2}, \frac{\sqrt{t \log \mathcal{N}_n}}{2F\kappa\sqrt{n}} \right\} \right\} dt. \end{aligned}$$

Here, the last inequality is by $r_j \geq \sqrt{\frac{\log \mathcal{N}_n}{n}}$. By letting $T = Cn \log \mathcal{N}_n$ for some constant $C \geq 4F^2\kappa^2/c'^2$, it is clear that when $t \geq T$, $\frac{t}{n\kappa^2} \geq \frac{\sqrt{t \log \mathcal{N}_n}}{2F\kappa\sqrt{n}}$, the inequality above can be written as

$$\mathbb{E}(|\xi_{\max}|^2 | (\mathbf{x}_i)_i) \leq Cn \log \mathcal{N}_n + \mathcal{N}_n \cdot \int_{Cn \log \mathcal{N}_n}^{+\infty} 2 \exp \left\{ -c' \frac{\sqrt{t \log \mathcal{N}_n}}{2F\kappa\sqrt{n}} \right\} dt.$$

Again by utilizing the equality $\int_{b^2}^{+\infty} e^{-\sqrt{t}a} dt = 2(ab + 1)e^{-ab}/a^2$ we conclude that as long as

$$C \geq 4F^2\kappa^2/c'^2,$$

$$\begin{aligned} \mathbb{E}(|\xi_{\max}|^2 | (\mathbf{x}_i)_i) &\leq Cn \log \mathcal{N}_n + \mathcal{N}_n \cdot \int_{Cn \log \mathcal{N}_n}^{+\infty} 2 \exp \left\{ -c' \frac{\sqrt{t \log \mathcal{N}_n}}{2F\kappa\sqrt{n}} \right\} dt \\ &= Cn \log \mathcal{N}_n + 4\mathcal{N}_n \left(\frac{c'\sqrt{C}}{F\kappa} \log \mathcal{N}_n + 1 \right) e^{-\frac{c'\sqrt{C}}{2F\kappa} \log \mathcal{N}_n} \cdot \frac{F^2\kappa^2n}{c'^2 \log \mathcal{N}_n} \\ &\leq 2Cn \log \mathcal{N}_n. \end{aligned}$$

By the definition of ξ_j in (B.9) and with $\xi_{\max} = \max_{j \in [\mathcal{N}]} \xi_j$, we have for any j' ,

$$\begin{aligned} \mathbb{E}^{1/2} \frac{\left| \sum_{i=1}^n \varepsilon_i (f_{j'}(\mathbf{x}_i) - f_0(\mathbf{x}_i)) \right|^2}{r_{j'}^2} &\leq \sqrt{\mathbb{E}(\mathbb{E}(|\xi_{\max}|^2 | (\mathbf{x}_i)_i))} \\ &\leq \sqrt{2Cn \log \mathcal{N}_n}. \end{aligned}$$

Combining the inequality above with (B.8), we have

$$\begin{aligned} \frac{1}{n} \left| \mathbb{E} \sum_{i=1}^n \varepsilon_i f_{j'}(\mathbf{x}_i) \right| &\leq \frac{1}{n} \left(\sqrt{\frac{\log \mathcal{N}_n}{n}} + \hat{R}_n^{1/2}(\tilde{f}, f_0)/\sqrt{c} + \tilde{\delta} \right) \cdot \sqrt{2Cn \log \mathcal{N}_n} \\ &\leq \sqrt{\frac{2C\hat{R}_n(\tilde{f}, f_0) \log \mathcal{N}_n}{n}} + \sqrt{2C} \left(\frac{\log \mathcal{N}_n}{n} + \sqrt{\frac{\log \mathcal{N}_n}{n}} \tilde{\delta} \right) \end{aligned} \quad (\text{B.10})$$

for some constant $C > 0$. Combining (B.10) with (B.7) we conclude that for any $\tilde{f} \in \mathcal{F}$,

$$\left| \mathbb{E} \frac{1}{n} \sum_{i=1}^n \varepsilon_i \tilde{f}(\mathbf{x}_i) \right| \leq \sqrt{\frac{2C\hat{R}_n(\tilde{f}, f_0) \log \mathcal{N}_n}{n}} + \sqrt{2C} \left(\frac{\log \mathcal{N}_n}{n} + \sqrt{\frac{\log \mathcal{N}_n}{n}} \tilde{\delta} \right) + 2\tilde{\delta}C$$

for some large constant $C > 0$, which completes the proof of Lemma B.2.

B.3 Proof of Lemma B.3

Recall the definition of $\Delta_n(\hat{f}_n, f_0)$

$$\Delta_n(\hat{f}_n, f_0) = \mathbb{E}_{f_0} \frac{1}{n} \sum_{i=1}^n -y_i \hat{f}_n(\mathbf{x}_i) + \psi(\hat{f}_n(\mathbf{x}_i)) - \inf_{f \in \mathcal{F}(L, \mathbf{p}, s, \mathcal{F})} \frac{1}{n} \sum_{i=1}^n -y_i f(\mathbf{x}_i) + \psi(f(\mathbf{x}_i)).$$

The first inequality we can obtain is, for any fixed $f \in \mathcal{F}$,

$$\mathbb{E} \frac{1}{n} \sum_{i=1}^n -y_i \hat{f}_n(\mathbf{x}_i) + \psi(\hat{f}_n(\mathbf{x}_i)) \leq \mathbb{E} \frac{1}{n} \sum_{i=1}^n -y_i f(\mathbf{x}_i) + \psi(f(\mathbf{x}_i)) + \Delta_n(\hat{f}_n, f_0). \quad (\text{B.11})$$

Note that f and f_0 are both fixed. For any $\mathbf{X} \stackrel{\mathcal{D}}{=} \mathbf{x}_i$, the inequality above further implies that

$$\hat{R}_n(\hat{f}_n, f_0) \leq \mathbb{E} \frac{1}{n} \sum_{i=1}^n \ell(\mathbf{x}_i; f, f_0) + \mathbb{E} \frac{1}{n} \sum_{i=1}^n \varepsilon_i \hat{f}_n(\mathbf{x}_i) + \Delta_n(\hat{f}_n, f_0)$$

$$\begin{aligned}
&= \mathbb{E}\ell(\mathbf{X}; f, f_0) + \mathbb{E} \frac{1}{n} \sum_{i=1}^n \varepsilon_i \hat{f}_n(\mathbf{x}_i) + \Delta_n(\hat{f}_n, f_0) \\
&\leq \inf_{f \in \mathcal{F}} \mathbb{E}\ell(\mathbf{X}; f, f_0) + \sqrt{\frac{2C \hat{R}_n(\hat{f}_n, f_0) \log \mathcal{N}_n}{n}} \\
&\quad + \sqrt{2C} \left(\frac{\log \mathcal{N}_n}{n} + \sqrt{\frac{\log \mathcal{N}_n}{n} \tilde{\delta}} \right) + 2\tilde{\delta}C + \Delta_n(\hat{f}_n, f_0).
\end{aligned}$$

Here, $\varepsilon_i = y_i - \psi'(f_0(\mathbf{x}_i))$. The first inequality is from (B.11), the first equality is by $\mathbb{E}\ell(\mathbf{X}; f, f_0) = \mathbb{E}\ell(\mathbf{x}_i; f, f_0)$ for any fixed $f \in \mathcal{F}$, and the last inequality is by Lemma B.2.

B.4 Proof of Lemma B.4

Let $\tilde{f} = \operatorname{argmin}_{f \in \mathcal{F}} \sum_{i=1}^n -y_i f(\mathbf{x}_i) + \psi(f(\mathbf{x}_i))$ be the global empirical risk estimator. We have the following decomposition, by letting $\varepsilon_i = y_i - \psi'(f_0(\mathbf{x}_i))$. That is,

$$\hat{R}_n(\hat{f}_n, f_0) - \hat{R}_n(\tilde{f}, f_0) = \Delta_n(\hat{f}_n, f_0) + \mathbb{E} \frac{1}{n} \sum_{i=1}^n \varepsilon_i \hat{f}_n(\mathbf{x}_i) - \mathbb{E} \frac{1}{n} \sum_{i=1}^n \varepsilon_i \tilde{f}(\mathbf{x}_i). \quad (\text{B.12})$$

From Lemma B.2, we have

$$\left| \mathbb{E} \frac{1}{n} \sum_{i=1}^n \varepsilon_i \tilde{f}(\mathbf{x}_i) \right| \leq \sqrt{\frac{2C \hat{R}_n(\tilde{f}, f_0) \log \mathcal{N}_n}{n}} + \sqrt{2C} \left(\frac{\log \mathcal{N}_n}{n} + \sqrt{\frac{\log \mathcal{N}_n}{n} \tilde{\delta}} \right) + 2\tilde{\delta}C$$

for any $\tilde{f} \in \mathcal{F}$ with some constant $C > 0$. Therefore (B.12) yields

$$\begin{aligned}
\hat{R}_n(\hat{f}_n, f_0) - \hat{R}_n(\tilde{f}, f_0) &\geq \Delta_n(\hat{f}_n, f_0) - \sqrt{\frac{2C \hat{R}_n(\hat{f}_n, f_0) \log \mathcal{N}_n}{n}} - \sqrt{\frac{2C \hat{R}_n(\tilde{f}, f_0) \log \mathcal{N}_n}{n}} \\
&\quad - 2\sqrt{2C} \left(\frac{\log \mathcal{N}_n}{n} + \sqrt{\frac{\log \mathcal{N}_n}{n} \tilde{\delta}} \right) - 4\tilde{\delta}C.
\end{aligned} \quad (\text{B.13})$$

For any $a, b > 0$, it holds that $2ab \leq \rho a^2 + b^2/\rho$ for any $\rho > 0$. By letting $a = \hat{R}_n(\hat{f}_n, f_0)$, $b = \hat{R}_n(\tilde{f}, f_0)$, $c = \sqrt{\frac{C \log \mathcal{N}_n}{2n}}$ and $d = \Delta_n(\hat{f}_n, f_0) - 2\sqrt{2C} \left(\frac{\log \mathcal{N}_n}{n} + \sqrt{\frac{\log \mathcal{N}_n}{n} \tilde{\delta}} \right) - 4\tilde{\delta}C$, (B.13) can be written as

$$\begin{aligned}
a - b &\geq d - 2\sqrt{ac} - 2\sqrt{bc} \\
&\geq d - \rho a - \frac{c^2}{\rho} - b - c^2
\end{aligned}$$

for any $\rho > 0$. We directly conclude that

$$a \geq \frac{d}{1 + \rho} - \frac{c^2}{1 + \rho},$$

which is

$$\widehat{R}_n(\widehat{f}_n, f_0) \geq \frac{1}{1+\rho} \cdot \left(\Delta_n(\widehat{f}_n, f_0) - 2\sqrt{2C} \left(\frac{\log \mathcal{N}_n}{n} + \sqrt{\frac{\log \mathcal{N}_n}{n}} \widetilde{\delta} \right) - 4\widetilde{\delta}C - \frac{C \log \mathcal{N}_n}{2n} \right).$$

This completes the proof of Lemma B.4.

B.5 Proof of Proposition A.1

We first prove the upper bound. From Lemma B.1, we can let $a_1 = \widehat{R}_n(\widehat{f}_n, f_0)$, $b_1 = R_n(\widehat{f}_n, f_0)$, $c_1 = \frac{R}{n} \sqrt{9n \log \mathcal{N}_n + 4n \frac{1+3 \log \mathcal{N}_n}{\log \mathcal{N}_n}}$ and $d_1 = \frac{2R(3 \log \mathcal{N}_n + 2)}{n} + 5\widetilde{\delta}C_{\text{Lip}}$. The inequality in Lemma B.1 can be written as

$$|a_1 - b_1| \leq 2\sqrt{a_1}c_1 + d_1. \quad (\text{B.14})$$

Furthermore, from Lemma B.3, we can let $a_2 = a_1 = \widehat{R}_n(\widehat{f}_n, f_0)$, $c_2 = \sqrt{\frac{C \log \mathcal{N}_n}{2n}}$ and $d_2 = \inf_{f \in \mathcal{F}} \mathbb{E} \ell(\mathbf{X}; f, f_0) + \sqrt{2C} \left(\frac{\log \mathcal{N}_n}{n} + \sqrt{\frac{\log \mathcal{N}_n}{n}} \widetilde{\delta} \right) + 2\widetilde{\delta}C + \Delta_n(\widehat{f}_n, f_0)$. The inequality in Lemma B.3 can be written as

$$a_2 \leq 2\sqrt{a_2}c_2 + d_2. \quad (\text{B.15})$$

From (B.14), we have, for any $0 < \rho_1 < 1$,

$$b_1 - a_1 \leq \rho_1 a_1 + \frac{c_1^2}{\rho_1} + d_1,$$

while (B.15) implies that, for any $\rho_2 > 0$,

$$a_2 \leq \rho_2 a_2 + \frac{c_2^2}{\rho_2} + d_2.$$

Setting $a_1 = a_2$ and combining the two inequalities above, we have

$$b_1 \leq (1 + \rho_1) \cdot \left(\frac{c_2^2}{(1 - \rho_2)\rho_2} + d_2 \right) + \frac{c_1^2}{\rho_1} + d_1.$$

By the definition of a_1 , b_1 , c_1 , d_1 , a_2 , c_2 and d_2 and by letting $\rho_1 = 1$ and $\rho_2 = 0.5$, we conclude that there exists a constant C' depending only on F , function ψ and κ such that

$$R_n(\widehat{f}, f_0) \leq 2\Delta_n(\widehat{f}_n, f_0) + 2 \inf_{f \in \mathcal{F}} \mathbb{E} \ell(\mathbf{X}; f, f_0) + C' \left(\frac{\log \mathcal{N}_n}{n} + \left(\sqrt{\frac{\log \mathcal{N}_n}{n}} + 1 \right) \widetilde{\delta} \right).$$

We complete the upper bound in Proposition A.1.

We then prove the lower bound in Proposition A.1. From Lemma B.4, we can let $a_3 = \widehat{R}_n(\widehat{f}_n, f_0)$, and have

$$a_1 = a_3 \geq \frac{1}{1+\rho} \cdot \left(\Delta_n(\widehat{f}_n, f_0) - 2\sqrt{2C} \left(\frac{\log \mathcal{N}_n}{n} + \sqrt{\frac{\log \mathcal{N}_n}{n}} \widetilde{\delta} \right) - 4\widetilde{\delta}C - \frac{C \log \mathcal{N}_n}{2n} \right). \quad (\text{B.16})$$

Hence, from (B.14) we have for any $0 < \rho_3 < 1$,

$$a_1 - b_1 \leq \rho_3 a_1 + \frac{c_1^2}{\rho_3} + d_1,$$

or

$$b_1 \geq (1 - \rho_3)a_1 - \frac{c_1^2}{\rho_3} - d_1.$$

We can let $\rho = 0.2$ in (B.16) and $\rho_3 = 0.4$, and it is easy to conclude that there exists a constant c' depending only on F , function ψ and κ such that

$$R_n(\hat{f}, f_0) \geq \frac{1}{2}\Delta_n(\hat{f}_n, f_0) - c' \left(\frac{\log \mathcal{N}_n}{n} + \left(\sqrt{\frac{\log \mathcal{N}_n}{n}} + 1 \right) \tilde{\delta} \right).$$

C Additional Numerical Results

We give some additional experiments by considering a different values of subsampling iterations B . While Theorems 3.7 and 3.8 assume $B \rightarrow \infty$ to eliminate the U-statistic variance asymptotically, in basic settings we have a smaller B for feasible computational burden. We empirically test the impact of finite B by comparing the larger choices $B = 3000$ against a small reference $B = 1400$.

Table 5: Simulation results for different models under varying sample sizes n and subsampling ratios r with $B=3000$.

	Bias _{f}	MAE _{f}	Bias _{ψ'}	MAE _{ψ'}	EmpSD	SE	CP	AIL
Logistic model								
$n = 400, r = n^{0.8}$	0.17	0.70(0.62)	0.01	0.10(0.11)	0.94	0.88	94.0%	0.42(0.22)
$r = n^{0.85}$	-0.01	0.65(0.57)	0.00	0.09(0.10)	0.86	0.84	93.9%	0.43(0.20)
$r = n^{0.9}$	-0.14	0.65(0.55)	-0.01	0.09(0.10)	0.85	0.79	93.2%	0.43(0.19)
Bootstrap with f_0	-0.43	1.03(0.82)	-0.05	0.15(0.14)	1.31	-	98.7%	0.82(0.14)
$n = 700, r = n^{0.8}$	0.24	0.68(0.55)	0.03	0.09(0.10)	0.87	0.83	93.2%	0.41(0.22)
$r = n^{0.85}$	0.05	0.61(0.50)	0.01	0.09(0.09)	0.79	0.76	93.9%	0.40(0.20)
$r = n^{0.9}$	-0.09	0.62(0.50)	0.00	0.09(0.08)	0.80	0.68	91.7%	0.39(0.17)
Bootstrap with f_0	-0.30	0.84(0.70)	-0.02	0.12(0.11)	1.10	-	93.9%	0.62(0.16)
Poisson Model								
$n = 400, r = n^{0.8}$	-0.20	0.38(0.33)	-0.37	0.48(0.50)	0.50	0.38	87.1%	1.68(0.99)
$r = n^{0.85}$	-0.14	0.36(0.32)	-0.29	0.45(0.47)	0.48	0.38	90.9%	1.88(1.15)
$r = n^{0.9}$	-0.08	0.34(0.32)	-0.22	0.44(0.45)	0.47	0.39	92.5%	2.08(1.34)
Bootstrap with f_0	0.10	0.47(0.43)	0.25	0.81(1.06)	0.64	-	95.0%	6.33(5.71)
$n = 700, r = n^{0.8}$	-0.09	0.33(0.32)	-0.22	0.39(0.38)	0.46	0.34	90.2%	1.59(0.83)
$r = n^{0.85}$	-0.02	0.31(0.32)	-0.14	0.36(0.35)	0.45	0.35	91.7%	1.76(0.96)
$r = n^{0.9}$	0.04	0.30(0.33)	-0.07	0.35(0.33)	0.45	0.36	93.2%	1.99(1.16)
Bootstrap with f_0	-0.02	0.42(0.42)	-0.12	0.55(0.54)	0.59	-	95.4%	4.71(3.54)
Binomial Model								
$n = 400, r = n^{0.8}$	0.40	0.61(0.54)	0.04	0.08(0.08)	0.81	0.57	85.2%	0.27(0.00)
$r = n^{0.85}$	0.31	0.55(0.48)	0.03	0.07(0.07)	0.73	0.59	90.3%	0.29(0.00)
$r = n^{0.9}$	0.23	0.50(0.43)	0.03	0.06(0.07)	0.66	0.61	93.2%	0.30(0.00)
Bootstrap with f_0	-0.00	0.78(0.69)	-0.02	0.10(0.10)	1.04	-	94.3%	0.53(0.23)
$n = 700, r = n^{0.8}$	0.09	0.40(0.38)	0.01	0.06(0.06)	0.55	0.43	89.5%	0.22(0.00)
$r = n^{0.85}$	0.04	0.38(0.35)	0.01	0.05(0.06)	0.52	0.44	90.9%	0.23(0.00)
$r = n^{0.9}$	0.00	0.37(0.34)	0.01	0.05(0.05)	0.51	0.45	91.6%	0.24(0.01)
Bootstrap with f_0	-0.12	0.54(0.44)	-0.02	0.07(0.08)	0.70	-	94.8%	0.39(0.18)

Table 5 reports the performance of our method with $B = 3000$. Consistent with earlier findings, we observe similar behavior across key metrics: (1) mean absolute error (MAE) for both $\psi'(\hat{f}^B)$ and \hat{f}^B remains low, (2) empirical standard deviations (empSD) and estimated standard errors (SE) stay closely aligned, (3) coverage probabilities (CP) are near 95% level and (4) comparable average interval lengths (AIL). This indicates that increasing B beyond a moderate threshold (e.g., $B = 1400$) yields minor improvement. Consequently, our proposed ESM achieves reliable inference performance when B is sufficiently large, with no need for excessive computation.